iScience

CellPress

Article

HNF4A Haploinsufficiency in MODY1 Abrogates Liver and Pancreas Differentiation from Patient-Derived Induced Pluripotent Stem Cells

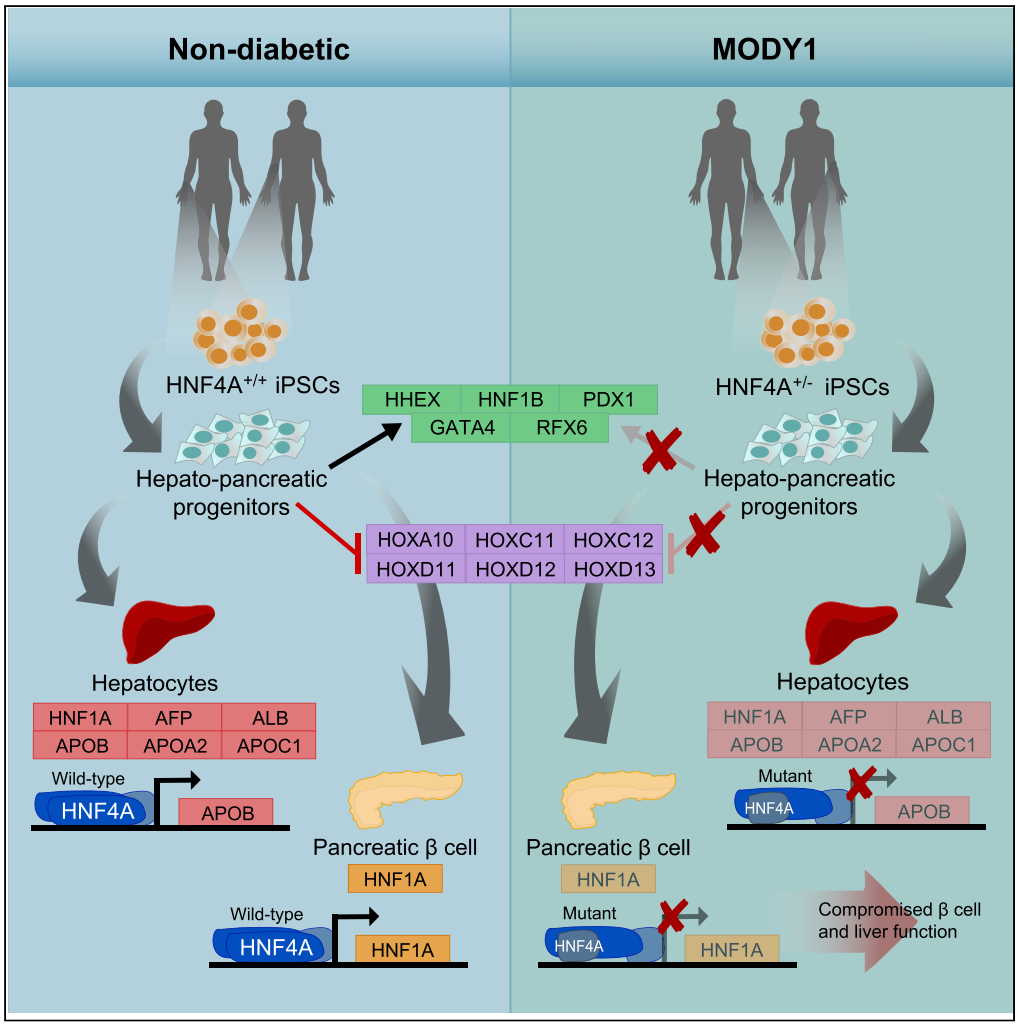

Natasha Hui Jin Ng, Joanita Binte Jasmen, Chang Siang Lim, ..., Ludovic Vallier, Shawn Hoon, Adrian Kee Keong Teo

drainteo@gmail.com

HIGHLIGHTS

HNF4A is downregulated and predominantly mislocalized in the cytoplasm in MODY1

Foregut markers, pancreatic and hepatic genes, were downregulated in MODY1-HPPs

A reciprocal upregulation of hindgut *HOX* genes was observed in MODY1-HPPs

Mutant HNF4A resulted in loss of transcriptional activation of target genes

Ng et al., iScience *16*, 192–205
June 28, 2019
https://doi.org/10.1016/j.isci.2019.05.032

iScience

CellPress

Article

HNF4A Haploinsufficiency in MODY1 Abrogates Liver and Pancreas Differentiation from Patient-Derived Induced Pluripotent Stem Cells

Natasha Hui Jin Ng,[1,10] Joanita Binte Jasmen,[1,10] Chang Siang Lim,[1] Hwee Hui Lau,[1,2] Vidhya Gomathi Krishnan,[3] Juned Kadiwala,[4] Rohit N. Kulkarni,[5] Helge Ræder,[6,7] Ludovic Vallier,[4,8] Shawn Hoon,[3] and Adrian Kee Keong Teo[1,2,9,11,*]

SUMMARY

Maturity-onset diabetes of the young 1 (MODY1) is a monogenic diabetes condition caused by heterozygous *HNF4A* mutations. We investigate how HNF4A haploinsufficiency from a MODY1/HNF4A mutation influences the development of foregut-derived liver and pancreatic cells through differentiation of human induced pluripotent stem cells from a MODY1 family down the foregut lineage. In MODY1-derived hepatopancreatic progenitors, which expressed reduced HNF4A levels and mislocalized HNF4A, foregut genes were downregulated, whereas hindgut-specifying *HOX* genes were upregulated. MODY1-derived hepatocyte-like cells were found to exhibit altered morphology. Hepatic and β cell gene signatures were also perturbed in MODY1-derived hepatocyte-like and β-like cells, respectively. As mutant HNF4A (p.Ile271fs) did not undergo complete nonsense-mediated decay or exert dominant negativity, HNF4A-mediated loss of function is likely due to impaired transcriptional activation of target genes. Our results suggest that in MODY1, liver and pancreas development is perturbed early on, contributing to altered hepatic proteins and β cell defects in patients.

INTRODUCTION

Maturity-onset diabetes of the young 1 (MODY1) is an autosomal dominant monogenic diabetes condition typically manifesting before the age of 25 years. This condition is caused by inactivating mutations in the hepatocyte nuclear factor 4A (*HNF4A*) gene (Yamagata et al., 1996) and is characterized by defects in glucose-stimulated insulin secretion (GSIS) from the pancreatic β cells (Byrne et al., 1995). Owing to the inaccessibility of human pancreatic tissue, rodent models have traditionally been used to study the molecular mechanisms underlying MODY1. Unfortunately, conditional knockout of *Hnf4a* in mouse pancreatic β cells did not result in a diabetic phenotype, although GSIS is impaired (Boj et al., 2010; Gupta et al., 2005; Miura et al., 2006). More importantly, *Hnf4a*$^{+/-}$ mice exhibit normal glucose tolerance (Stoffel and Duncan, 1997), indicating that rodent models do not accurately recapitulate the MODY1 phenotype in humans. Human induced pluripotent stem cell (hiPSC)-based disease modeling strategies (Teo et al., 2013a) therefore provide opportunities to investigate the impact of MODY1/*HNF4A* mutation on the development of the foregut lineage in humans. In particular, the ventral foregut endoderm gives rise to progenitors that subsequently form the liver, whose development and function is heavily dependent on regulation by HNF4A, or the pancreatic β cells, which are known to be implicated in MODY1 pathophysiology.

HNF4A is a member of the steroid hormone receptor superfamily and functions as a transcription factor upon homodimerization (Sladek et al., 1990). Its expression is regulated by either the P1 (proximal) or P2 (distal) promoter. The usage of alternate promoters and presence of alternative splicing results in up to 12 known *HNF4A* isoforms that are expressed in a developmental stage- and tissue-specific manner (Eeckhoute et al., 2003a; Harries et al., 2008; Huang et al., 2009; Jiang et al., 2003; Tanaka et al., 2006). Therefore *HNF4A* expression is dynamically regulated to ensure proper formation and function of multiple organs, in particular, the liver and pancreas (Lau et al., 2018), which are the tissues we focus on in our study.

Knockout of *Hnf4a* in mice is dispensable for early development of the liver, whereas it is required for driving hepatic specification at later stages and in maintaining proper liver function (Li et al., 2000). In an early human pluripotent stem cell differentiation study, *HNF4A* was found to be necessary for establishing the hepatic gene regulatory network and induction of hepatic cell fate (DeLaForest et al., 2011). This

[1]Stem Cells and Diabetes Laboratory, Institute of Molecular and Cell Biology, A*STAR, Singapore 138673, Singapore

[2]School of Biological Sciences, Nanyang Technological University, Singapore 637551, Singapore

[3]Molecular Engineering Lab, A*STAR, Singapore 138673, Singapore

[4]Wellcome Trust-Medical Research Council Cambridge Stem Cell Institute, Anne McLaren Laboratory, Department of Surgery, University of Cambridge, Cambridge CB2 0SZ, UK

[5]Section of Islet Cell and Regenerative Biology, Joslin Diabetes Center, Harvard Stem Cell Institute, Department of Medicine, Brigham and Women's Hospital, and Harvard Medical School, Boston, MA 02215, USA

[6]Department of Pediatrics, Haukeland University Hospital, 5021 Bergen, Norway

[7]KG Jebsen Center for Diabetes Research, Department of Clinical Science, Faculty of Medicine, University of Bergen, 5020 Bergen, Norway

[8]Wellcome Trust Sanger Institute, Hinxton CB10 1SA, UK

[9]Department of Biochemistry and Department of Medicine, Yong Loo Lin School of Medicine, National University of Singapore, Singapore 117596, Singapore

[10]These authors contributed equally

[11]Lead Contact

*Correspondence: drainteo@gmail.com

https://doi.org/10.1016/j.isci.2019.05.032

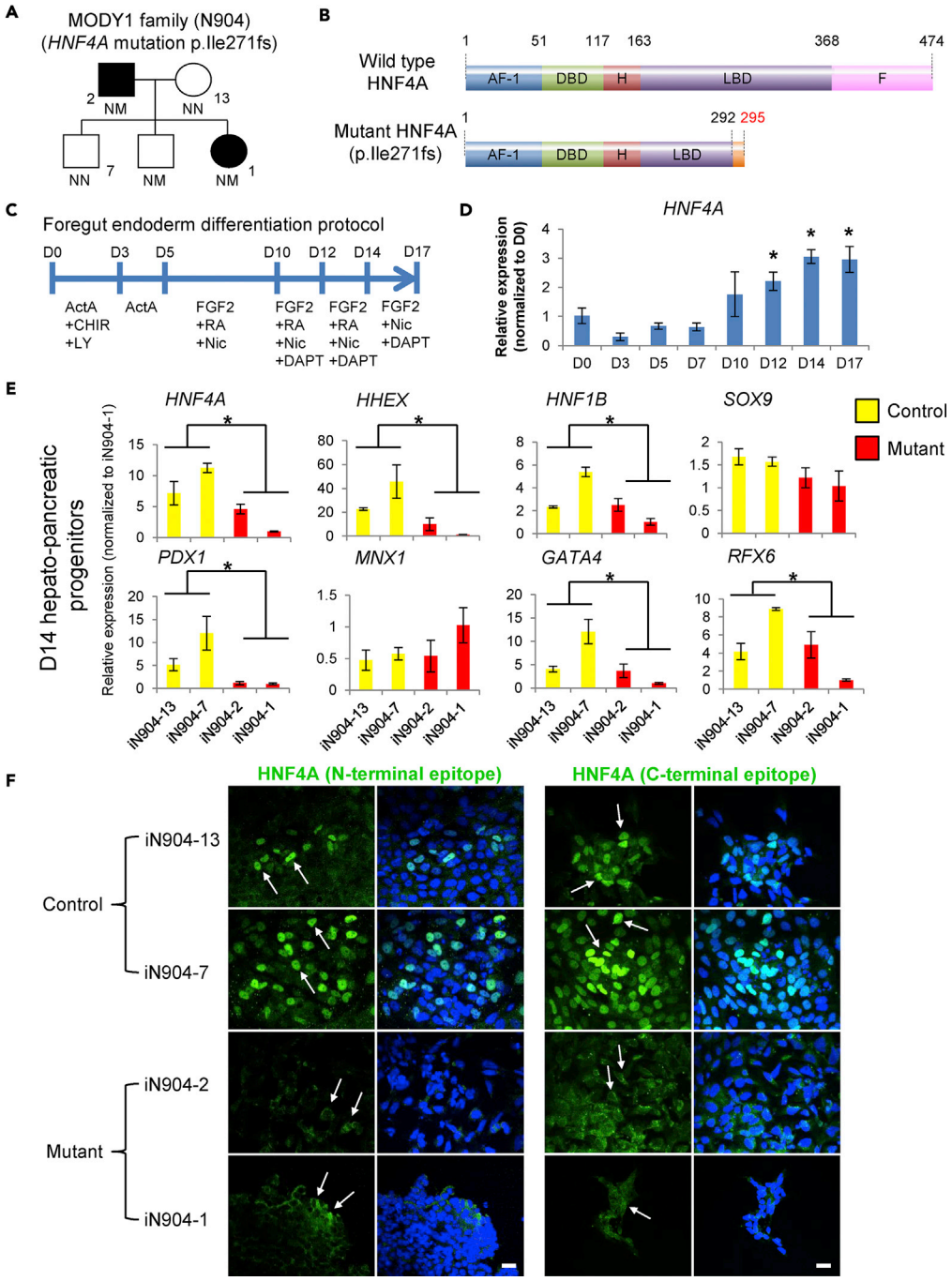

Figure 1. *HNF4A* Mutation (p.Ile271fs) Causes Impaired Foregut/Early Hepatopancreatic Progenitor (HPP) Development

(A) MODY1 family node showing non-diabetic control-hiPSCs (iN904-13 and iN904-7) and MODY1-hiPSCs (iN904-2 and iN904-1).

(B) p.Ile271fs mutation results in C-terminally truncated HNF4A that lacks part of the ligand-binding domain (LBD) and the entire F repressor domain (not drawn to scale).

(C) The 17-day differentiation protocol for generating foregut endoderm and HPPs.

(D) qPCR analysis of *HNF4A* expression during HPP differentiation.

(E) qPCR analyses of *HNF4A* transcripts and foregut endoderm markers such as *HHEX, HNF1B, PDX1, GATA4, and RFX6* in control and MODY1-HPPs.

Figure 1. *Continued*

(F) Immunofluorescent confocal images showing the localization of HNF4A protein in control and MODY1-HPPs, based on antibodies targeting the N- or C-terminal regions of HNF4A. Blue, DAPI; green, HNF4A; scale bars, 50 μm. White arrows point to the nuclear or cytoplasmic localization signal of HNF4A. Confocal images were acquired using similar scan settings across samples.

Data are represented as mean ± SD of n = 3; representative of three independent experiments. *$p < 0.05$ versus D0 or control samples by Student's t test. See also Figures S1 and S2.

correlates with the observation that patients with an inactivating *HNF4A* mutation exhibit alterations in liver function (Gardner and Tai, 2012; Pearson et al., 2005; Shih et al., 2000). In addition to the liver, Hnf4a is also expressed in the maturing pancreas in mice and is largely confined to the developing islet and acinar cells (Nammo et al., 2008). A recent study showed that MODY1/*HNF4A* mutation does not prevent formation of INS^+ cells from *in vitro* differentiations (Vethe et al., 2017). Nonetheless, the molecular and transcriptional impacts of heterozygous *HNF4A* mutation on early foregut endoderm, liver, and pancreas development leading to disease onset in humans remain largely unexplored.

We hypothesized that the MODY1/*HNF4A* mutation affects early human foregut development that can potentially lead to both liver and pancreas developmental defects. To circumvent the lack of access to human tissues during early development, we generated hiPSCs from members of a MODY1 family (with and without heterozygous *HNF4A* mutation) and differentiated them into hepatopancreatic foregut endoderm (henceforth termed *hepatopancreatic progenitors* [HPPs]), as well as hepatic and pancreatic β-like cells using independent, established protocols. Our data indicate that *HNF4A* haploinsufficiency, as a result of a loss-of-function MODY1 mutation, affects early human foregut development and that this deficiency is propagated to both hepatic and pancreatic cell fates. Our human disease model provides a platform for investigating why patients with MODY1 have specific hepatic and β cell developmental defects.

RESULTS

Establishing a MODY1 Disease Model Using Patient-Derived iPSCs

We previously reported the recruitment of two members of a MODY1 family harboring a heterozygous p.Ile271fs mutation in HNF4A (Figure 1A) (Teo et al., 2013b) resulting in premature truncation of the protein (Figure 1B). To facilitate rigorous and comprehensive hiPSC-based MODY1 disease modeling, we recruited more members of the same family and rederived a total of nine hiPSC lines composed of MODY1-hiPSCs from two patients (iN904-2 and iN904-1A/B/C) and control-hiPSCs from two non-diabetic family members (iN904-13A/B and iN904-7A/B/C) (Figures 1A and S1). Using a previously published 17-day foregut endoderm differentiation protocol, we observed that *HNF4A* expression peaked at day 14 (D14) (Figures 1C and 1D) (Teo et al., 2015b, 2016), and that ~70% of D14 HPPs were $HNF4A^+$ (Figure S2A), thereby providing a suitable model for studying *HNF4A* gene function and disease mechanisms underlying MODY1.

HNF4A Mutation (p.Ile271fs) Causes Impaired Foregut/Early HPP Development

To elucidate the effects of the p.Ile271fs mutation, we simultaneously differentiated control- and MODY1-hiPSCs into HPPs. Both control- and MODY1-hiPSCs were able to differentiate into definitive endoderm cells at day 3 of differentiation (Figure S2B). At D14 of differentiation, although we observed no obvious morphological differences between control- and MODY1-HPPs (Figure S2C), the MODY1-HPPs expressed significantly lower levels of total *HNF4A* (Figure 1E). In fact, wild-type (WT) HNF4A protein was expressed at markedly lower levels in MODY1-HPPs based on protein expression data despite the presence of one copy of the WT allele at *HNF4A* (Figure S2D). To determine if P1- or P2-driven *HNF4A* transcripts were affected, we carried out isoform-specific qPCR analyses and showed that both P1- and P2-driven forms of *HNF4A* are potentially affected in the D14 HPPs (Figure S2E).

We further detected lower levels of foregut endoderm genes *HHEX*, *HNF1B*, *PDX1*, *GATA4*, and *RFX6* in the MODY1-HPPs, whereas no differences were observed for other pancreas-related genes *SOX9* or *MNX1* (Figure 1E), reflecting a downregulation of specific gene targets of *HNF4A* affected by the p.Ile271fs mutation rather than a global downregulation of pancreatic developmental genes. Downregulation of PDX1 and GATA4 was confirmed at protein level by immunofluorescence staining (Figure S2F). Subsequent immunofluorescence analyses additionally revealed that HNF4A protein is largely sequestered in the cytoplasm of the MODY1-HPPs as opposed to the predominant nuclear localization observed in control-HPPs

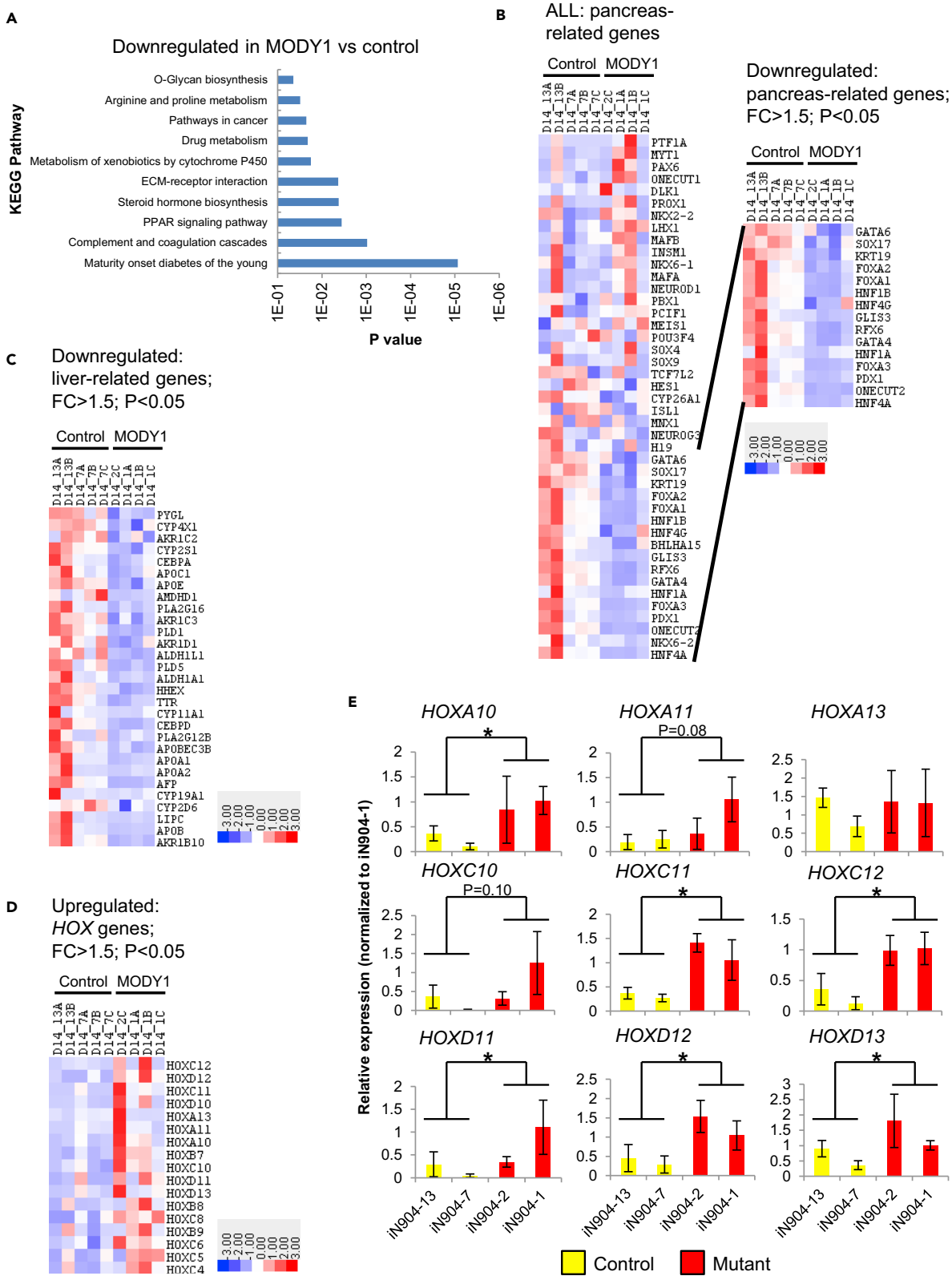
A
Downregulated in MODY1 vs control
KEGG Pathway
O-Glycan biosynthesis
Arginine and proline metabolism
Pathways in cancer
Drug metabolism
Metabolism of xenobiotics by cytochrome P450
ECM-receptor interaction
Steroid hormone biosynthesis
PPAR signaling pathway
Complement and coagulation cascades
Maturity onset diabetes of the young
1E-01
1E-02
1E-03
1E-04
1E-05
1E-06
P value
B
ALL: pancreas-related genes
Control
MODY1
D14_13A
D14_13B
D14_7A
D14_7B
D14_7C
D14_2C
D14_1A
D14_1B
D14_1C
PTF1A
MYT1
PAX6
ONECUT1
DLK1
PROX1
NKX2-2
LHX1
MAFB
INSM1
NKX6-1
MAFA
NEUROD1
PBX1
PCIF1
MEIS1
POU3F4
SOX4
SOX9
TCF7L2
HES1
CYP26A1
ISL1
MNX1
NEUROG3
H19
GATA6
SOX17
KRT19
FOXA2
FOXA1
HNF1B
HNF4G
BHLHA15
GLIS3
RFX6
GATA4
HNF1A
FOXA3
PDX1
ONECUT2
NKX6-2
HNF4A
Downregulated: pancreas-related genes; FC>1.5; P<0.05
Control
MODY1
GATA6
SOX17
KRT19
FOXA2
FOXA1
HNF1B
HNF4G
GLIS3
RFX6
GATA4
HNF1A
FOXA3
PDX1
ONECUT2
HNF4A
3.00
2.00
1.00
0.00
1.00
2.00
3.00
C
Downregulated: liver-related genes; FC>1.5; P<0.05
Control
MODY1
PYGL
CYP4X1
AKR1C2
CYP2S1
CEBPA
APOC1
APOE
AMDHD1
PLA2G16
AKR1C3
PLD1
AKR1D1
ALDH1L1
PLD5
ALDH1A1
HHEX
TTR
CYP11A1
CEBPD
PLA2G12B
APOBEC3B
APOA1
APOA2
AFP
CYP19A1
CYP2D6
LIPC
APOB
AKR1B10
3.00
2.00
1.00
0.00
1.00
2.00
3.00
D
Upregulated: HOX genes; FC>1.5; P<0.05
Control
MODY1
HOXC12
HOXD12
HOXC11
HOXD10
HOXA13
HOXA11
HOXA10
HOXB7
HOXC10
HOXD11
HOXD13
HOXB8
HOXC8
HOXB9
HOXC6
HOXC5
HOXC4
3.00
2.00
1.00
0.00
1.00
2.00
3.00
E
HOXA10
HOXA11
HOXA13
HOXC10
HOXC11
HOXC12
HOXD11
HOXD12
HOXD13
*
P=0.08
P=0.10
Relative expression (normalized to iN904-1)
iN904-13
iN904-7
iN904-2
iN904-1
Control
Mutant

Figure 2. RNA Sequencing Analyses Reveal Global Transcriptional Changes Induced by the *HNF4A* Mutation in MODY1-HPPs at D14

(A–C) (A) Analysis of downregulated genes via the KEGG pathway. Heatmap analyses of (B) pancreas-related and (C) liver-related genes that are downregulated with fold change (FC) > 1.5, $p < 0.05$.

(D) Heatmap analyses of numerous caudal *HOX* genes involved in hindgut specification that are upregulated with FC > 1.5, $p < 0.05$. Colors in the heatmap depict gene expression in units of SD from the mean across all samples (upregulation in red, downregulation in blue). Controls indicated as 13A, 13B, 7A, 7B, and 7C; MODY1 indicated as 2, 1A–1C.

(E) qPCR analyses of caudal *HOX* gene expression in control and MODY1-HPPs.

Data are represented as mean ± SD of n = 3, representative of four independent experiments. *$p < 0.05$ versus control samples by Student's t test. See also Figure S3 and Table S1.

(Figure 1F). Mislocalization of the HNF4A protein could further account for the loss of its function as a transcription factor.

RNA Sequencing Analyses Reveal Downregulation of Pancreas- and Liver-Related Genes and Upregulation of Caudal *HOX* Genes

To thoroughly evaluate the genome-wide effects of the MODY1 mutation on foregut development, we performed RNA sequencing analyses on control and MODY1-hiPSC-derived D14 HPPs. Kyoto Encyclopedia of Genes and Genomes (KEGG) pathway analyses revealed that genes involved in MODY and numerous liver functions were significantly downregulated (Figure 2A), consistent with the known functions of HNF4A target genes (Bolotin et al., 2010; Odom et al., 2004). The affected genes were involved in processes related to steroid metabolism and lipoprotein and sterol binding and transport (Figure S3A), providing clues to the role of HNF4A target genes. On the other hand, genes involved in DNA binding, transcription factor, and channel activity were upregulated, possibly due to compensatory regulatory mechanisms (Figure S3B).

Heatmap analyses revealed that a subset of pancreas-related genes was downregulated in MODY1-HPPs (fold change [FC] > 1.5; $p < 0.05$) (Figure 2B), including *PDX1*, the *FOXA* gene family, *GATA4*, *RFX6*, *HNF1B*, *KRT19*, and *SOX17*. In addition, numerous hepatic genes such as the apolipoprotein (*APO*) genes, *AFP*, *TTR*, and *HHEX* were also downregulated in the MODY1-HPPs (Figure 2C), consistent with findings from *Hnf4a*$^{-/-}$ mice (Li et al., 2000). In contrast, we were intrigued to observe an upregulation of numerous caudal *HOX* genes including *HOXA10*, *HOXC11*, *HOXC12*, *HOXD11*, *HOXD12*, and *HOXD13* in the MODY1-HPPs (Figures 2D, 2E, and S3C). Although some of the changes were modest, likely due to the fact that the HPP protocol is suited for foregut, but not hindgut, differentiation, the trend toward increased levels of hindgut markers suggests a potential switch away from foregut specification. Indeed, these caudal *HOX* genes are typically upregulated only in differentiation conditions favorable for hindgut formation (high fibroblast growth factor 2 concentration) (Ameri et al., 2010) in which hindgut marker *CDX2* is upregulated, but not foregut marker *HNF4A* (Figure S3D). The loss of the repressor domain in HNF4A owing to the p.Ile271fs-truncating mutation may account for this "derepression" phenomenon.

MODY1-Mediated Loss of HNF4A Transcriptional Function Affects Subsequent Hepatic and Pancreatic Development Signatures

Following the *HNF4A* loss-of-function observations in the HPPs, which are representative of a progenitor stage, we next investigated impacts on subsequent tissue development. We used established differentiation protocols that aimed to direct the differentiation of the hiPSCs into hepatocytes or pancreatic β-like cells (Hannan et al., 2013; Pagliuca et al., 2014), as these are more representative of the liver and β cell differentiation process. First, time course differentiation of control-hiPSCs into hepatocyte-like cells (Hannan et al., 2013) revealed that *HNF4A* expression peaked on day 8 (D8), when 70%–80% HNF4A^{+} cells may be obtained, whereas other hepatic genes displayed peak expression on days 16 (D16) or 24 (D24) (Figures 3A and S4A).

During hepatic differentiation, we noted that control-hiPSCs formed polygonal hepatocyte-like cells, whereas MODY1-hiPSCs did not (Figure S4B). In addition, MODY1 hepatic progenitors expressed significantly lower levels of *HNF4A* and *HHEX* on D8, leading to reduced expression of *HNF1A* and hepatoblast marker *AFP* on D16, and finally reduced levels of key mature hepatocyte markers *APOA2*, *APOB*, *APOC1*, *APOE*, and *ALB* on D24 as opposed to control cells (Figure 3B). Residual HNF4A protein expressed in the MODY1 hepatic progenitors appeared to localize largely to the cytoplasm when compared with the controls (Figure S4), mirroring our earlier observations in the HPPs (Figure 1F). These data indicated that the early *HNF4A* loss-of-function effects (despite having a WT *HNF4A* allele) propagated into longer-term consequences that affected subsequent hepatic differentiation. This is consistent with the effects

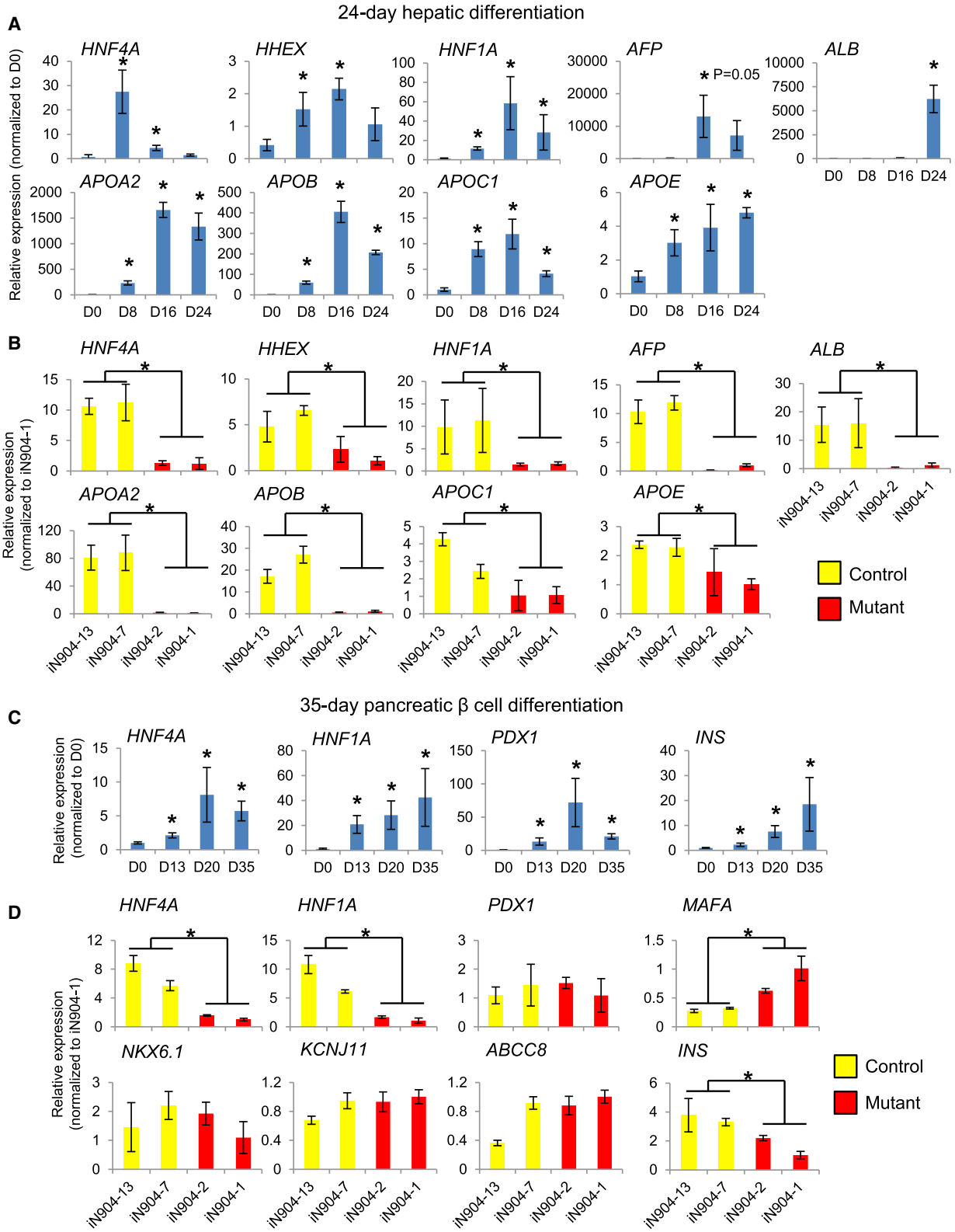
A
24-day hepatic differentiation
Relative expression (normalized to D0)
HNF4A
HHEX
HNF1A
AFP
* P=0.05
ALB
APOA2
APOB
APOC1
APOE
D0 D8 D16 D24
B
Relative expression (normalized to iN904-1)
iN904-13 iN904-7 iN904-2 iN904-1
Control
Mutant
C
35-day pancreatic β cell differentiation
Relative expression (normalized to D0)
PDX1
INS
D0 D13 D20 D35
D
MAFA
NKX6.1
KCNJ11
ABCC8

Figure 3. MODY1-Mediated *HNF4A* Haploinsufficiency in Early Foregut Development Affects Subsequent Hepatic and Pancreatic Development Signatures

(A and B) (A) qPCR analyses showing pattern of hepatic gene expression over a 24-day differentiation in control-hiPSC-derived hepatic cells and (B) comparison of hepatic gene expression changes between control and MODY1 hepatic cells.

(C and D) (C) qPCR analyses showing pattern of pancreatic β cell gene expression over a 35-day differentiation in control-hPSC-derived pancreatic β-like cells and (D) comparison of β cell gene expression changes between control and MODY1 pancreatic β-like cells.

Data are represented as mean ± SD of n = 3, representative of three independent experiments. *p < 0.05 versus control samples by Student's t test. See also Figure S4.

of shRNA-mediated knockdown of *HNF4A* in hPSCs that was reported previously (DeLaForest et al., 2011), although it is worth noting that a complete knockout of *HNF4A* in humans does not exist naturally.

We next investigated the impact of MODY1/*HNF4A* mutation on pancreatic β cell development using a published protocol for generating pancreatic β-like cells (Pagliuca et al., 2014). In differentiated WT β-like cells, *HNF4A* expression increased progressively over 35 days, together with other critical β cell transcripts such as *HNF1A*, *PDX1*, and *INS* (Figure 3C). Again, no difference was detected between the specification of control and MODY1 iPSCs into definitive endoderm cells, before the rise in HNF4A expression (Figure S4D). However, in MODY1 β-like cells both *HNF4A* and *HNF1A* were significantly downregulated, although this was not the case for a number of other β cell genes tested at D35 (Figure 3D). Despite some reduction in *INS* transcript levels in MODY1-derived β-like cells (Figure 3D), we could detect the expression of C-peptide in both control- and MODY1-derived β-like cells (Figure S4E). To corroborate the results observed in the MODY1-HPPs (Figure 1E), we also assessed gene expression changes in the pancreatic progenitors generated using the 35-day β cell differentiation protocol. We observed that the expression of *PDX1* and other progenitor markers was indeed reduced in the D13 pancreatic progenitors (Figure S4F), although PDX1 reduction at protein level was not always consistently observed (Figure S4G). We postulate that the early perturbations may be less apparent later in the differentiation owing to the exogenous stimuli that drive the differentiation of *PDX1*- and *INS*-expressing cells during β cell differentiation. Nonetheless, it was clear from our multiple differentiated cell models that loss in both *HNF4A* and *HNF1A* function in early hepatic and β cell development may contribute to the impaired tissue function in MODY1.

We then sought to define the molecular impact of HNF4A p.Ile271fs on its downstream targets including *HNF1A*, by evaluating the transcriptional potential of WT and mutant HNF4A in our hiPSC-derived hepatic differentiation models. As both P1- and P2-driven transcripts are present during foregut development (Figure S2E), the effects of both WT and mutant HNF4A2 and HNF4A8 (longest isoforms representative of P1- and P2-driven expression, respectively) were evaluated. When expressed in the D8 hepatic progenitors, WT HNF4A2 significantly activated *HNF1A* promoter activity, whereas mutant HNF4A did not elicit the same effect (Figure 4A). Similarly, in the D16 hepatic progenitors, WT but not mutant HNF4A2 resulted in activation of the *APOB* promoter and *AFP* enhancer (containing a HNF4A-binding motif) (Nakabayashi et al., 2004) (Figures 4B and 4C). The activation of the *AFP* enhancer by WT, but not mutant HNF4A2, was further replicated in HepG2 cells (Figure 4D), an AFP-producing human hepatoma cell line (Kawai et al., 2001). The lack of activation by mutant HNF4A may be explained in part by the reduced protein expression levels of mutant HNF4A compared with WT, although both HNF4A2/8 WT and mutants localized to the nuclei in the overexpression studies (Figures S5A and S5B). In all experiments, WT HNF4A8 exhibited a weaker transactivation potential when compared with HNF4A2, and in the case of the *HNF1A* promoter and *AFP* enhancer, the effect was only significant in MODY1-derived cells where endogenous HNF4A function is reduced (Figures 4A and 4C).

We further set out to investigate the regulation of *HNF1A* by HNF4A WT or mutants in human pancreatic β cells. As the suspension cell clumps generated from the pancreatic β cell differentiation were less amenable for *in vitro* assays unlike monolayer differentiation cultures, we used the human β cell line EndoC-βH1. Chromatin immunoprecipitation analyses in EndoC-βH1 showed that HNF4A was bound to the *HNF1A* promoter (Figure 4E), and subsequent knockdown of *HNF4A* by ~55% resulted in a corresponding reduction in *HNF1A* promoter activation (Figures 4F and 4G). This effect could be rescued by WT HNF4A overexpression but not mutant HNF4A (Figure 4G). Overall, we have shown that HNF4A directly regulates the transcription of key components of developing hepatic and pancreatic β cells, and that the MODY1/HNF4A mutation (p.Ile271fs) results in the inability to activate target promoters. Our patient-derived iPSC-based model thus provides an *in vitro* platform for the interrogation of the underlying disease mechanisms in the hepatic and β cells.

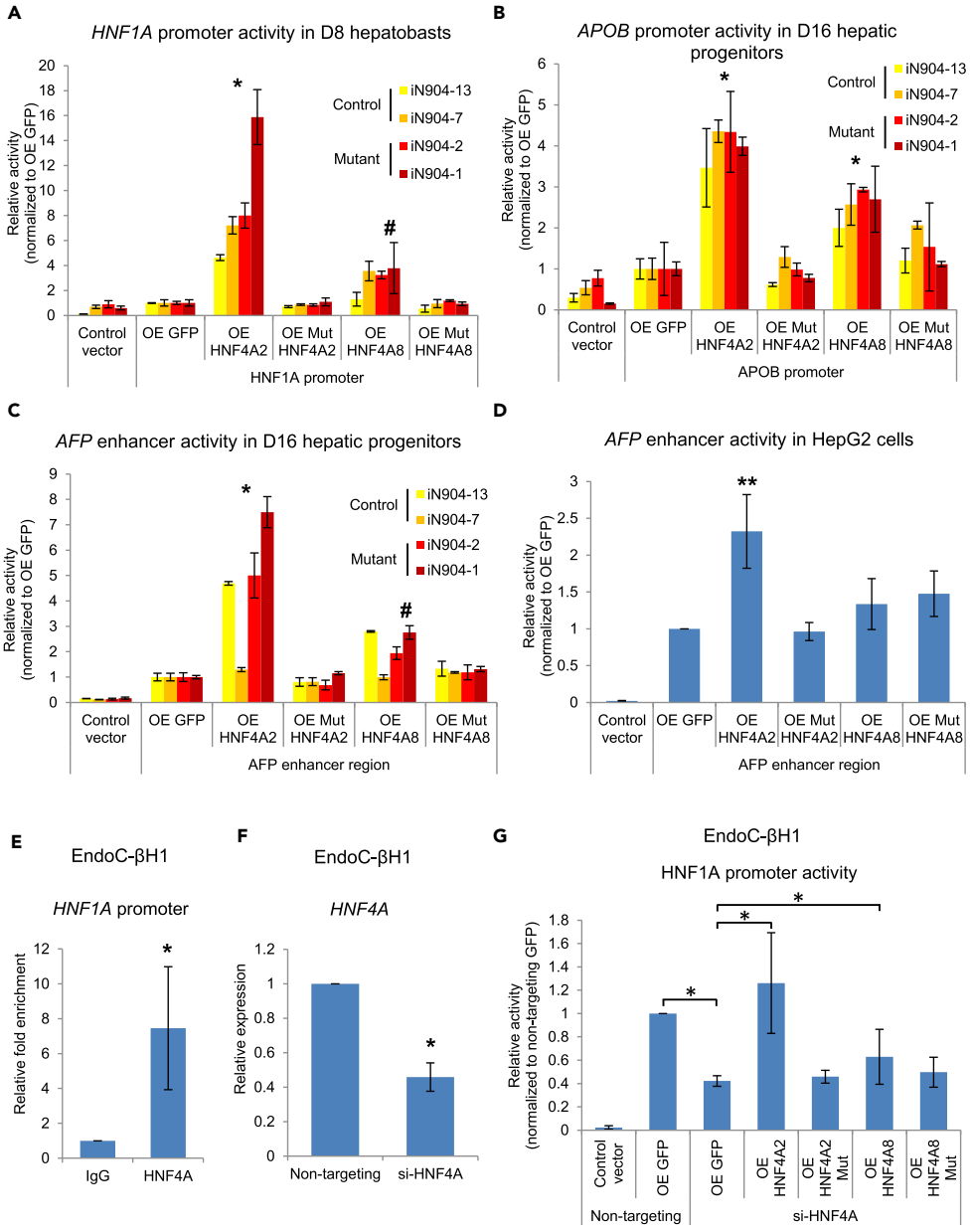

Figure 4. MODY1/HNF4A Mutation Results in Loss of Ability to Activate Downstream Target Promoters in Hepatic and Pancreatic β Cells

(A–D) Luciferase assays were performed to evaluate effects of WT or p.Ile271fs (Mut) HNF4A on the (A) *HNF1A* promoter, (B) *APOB* promoter, (C) *AFP* enhancer activity in hiPSC-derived hepatic cells, or (D) HepG2 cells. For (A–C), data are represented as mean ± SD n = 3, representative of two independent experiments. For (D), data are represented as mean ± SD of n = 12 from three independent experiments. *$p < 0.05$ versus GFP control in all hiPSC lines by two-way ANOVA; #$p < 0.05$ versus GFP control in mutant hiPSC lines only by two-way ANOVA. **$p = 0.01$ versus GFP control by Student's t test.

(E) Chromatin immunoprecipitation qPCR analysis of HNF4A binding onto *HNF1A* promoter in EndoC-βH1 cells.

(F) Small interfering RNA-mediated knockdown of *HNF4A* in EndoC-βH1 cells.

(G) Luciferase assay evaluating *HNF1A* promoter activity upon knockdown of *HNF4A* and rescue. For (E–G), data are represented as mean ± SD of n = 12 from three to four independent experiments. *$p < 0.05$ versus IgG/GFP control as indicated by Student's t test.

See also Figure S5.

MODY1 hiPSC-Derived Cells Express Both WT and Mutant *HNF4A* Transcripts and Do Not Exhibit Dominant Negativity

Finally, we sought to address the question of why the decrease in total *HNF4A* levels in MODY1-derived cells is beyond the expected 2-fold change given the presence of a WT allele in heterozygote carriers. We first determined the expression of WT and mutant *HNF4A* (p.Ile271fs) transcripts using a custom-designed allele-specific assay (Figure S5C). As observed across multiple differentiated cell types, both WT and mutant *HNF4A* transcripts are expressed in the MODY1-derived cells, confirming heterozygosity at mRNA level (Figures 5A–5C). The detection of mutant transcripts indicated that there is an absence of complete nonsense-mediated decay (NMD) of the nonsense mutant transcripts (Zhang et al., 2009). Next, we checked if the MODY1 mutation could result in a dominant negative effect by co-expressing WT and mutant HNF4A to recapitulate a heterozygous condition. Gene regulatory assays showed that WT HNF4A was able to activate *AFP* enhancer activity normally in the presence of mutant protein, suggesting a lack of dominant negativity (Figure 5D). Given that HNF4A is also known to occupy its own promoter (Bolotin et al., 2010; Odom et al., 2004), we performed further gene regulatory assays involving both the *HNF4A* P1 and P2 promoters and demonstrated that HNF4A can activate both promoters and subsequently its own expression in a feedforward manner (Figure 5E). Therefore loss of HNF4A function or mislocalization may result in failure to undergo autoregulation, accounting for overall reduced HNF4A expression in MODY1.

DISCUSSION

Earlier studies have reported *HNF4A* nonsense or missense gene mutations leading to either a loss-of-function or a dominant negative effect (Laine et al., 2000; Lausen et al., 2000; Sladek et al., 1998). The p.Ile271fs mutation in our study introduces a frameshift and premature stop codon, which could lead to generation of unstable mRNA that may to some degree be degraded by NMD (Frischmeyer and Dietz, 1999), accounting for the overall lowered *HNF4A* levels in MODY1-hiPSC-derived cells. However, we did not observe complete NMD given that mutant transcripts were detectable in our MODY1-derived cells. At protein level, crystallographic studies have reported that several key residues of the ligand-binding domain are involved in charge-driven interactions that improve dimerization. Mutations in this region such as p.Ile271fs may therefore affect the formation of functional homodimers and impair DNA-binding activity, thereby abolishing transcriptional activity or coactivator recruitment (Eeckhoute et al., 2003b; Ek et al., 2005; Hani et al., 1998; Stoffel and Duncan, 1997) to affect downstream gene regulation. Our work conclusively showed that loss of HNF4A-mediated gene regulation due to the p.Ile271fs mutation in a heterozygous state in MODY1 affected foregut endoderm gene expression signatures.

Our observations on caudal *HOX* gene upregulation led us to hypothesize that HNF4A typically functions to suppress ectopic hindgut *HOX* gene expression to facilitate proper foregut endoderm development, whereas this suppressive effect is disrupted in cells carrying the p.Ile271fs mutation. Further studies are required to determine whether *HOX* gene derepression is indirect, or if HNF4A requires other co-factors for its repressor function. Future work should also determine whether p.Ile271fs affects the specific interaction of HNF4A with ligands or co-factors important for its function. We propose that the impact of HNF4A haploinsufficiency on the specification of the foregut versus hindgut lineage is cell autonomous given the well-established function of HNF4A as a transcription factor. Nonetheless, the possibility of non–cell autonomy cannot be ruled out as previous studies have provided evidence for non-cell-autonomous functions of homeobox genes and other early developmental genes (Balbinot et al., 2018; Becker et al., 2016). Future experiments that involve fluorescent labeling of the WT and mutant MODY1 hiPSCs followed by differentiation and fluorescence-activated cell sorting analyses may shed light on this.

HNF4A has been reported to be important for rodent hepatocyte development (Li et al., 2000) and is essential for specifying the early hepatic differentiation program (DeLaForest et al., 2011). However, the impact of MODY1/*HNF4A* mutation on hepatic development in humans has not been explored, given the intractability of human liver tissue. Here, we capitalize on our patient-derived iPSCs and ability to differentiate them into multiple relevant cell types to model cell-type-specific phenotypes and investigate underlying disease mechanisms. Our results indicated that the early loss of *HNF4A* expression in hepatoblasts propagated to long-term consequences on hepatic cell fate, as seen in the reduced expression of *ALB* and numerous *APO* genes. This is consistent with observations that patients with MODY1 with an inactivating HNF4A mutation exhibit reduced secretion of hepatocyte-specific proteins such as APOs (Lehto et al., 1999; Pearson et al., 2005; Shih et al., 2000). Nonetheless, these alterations in liver function may not be

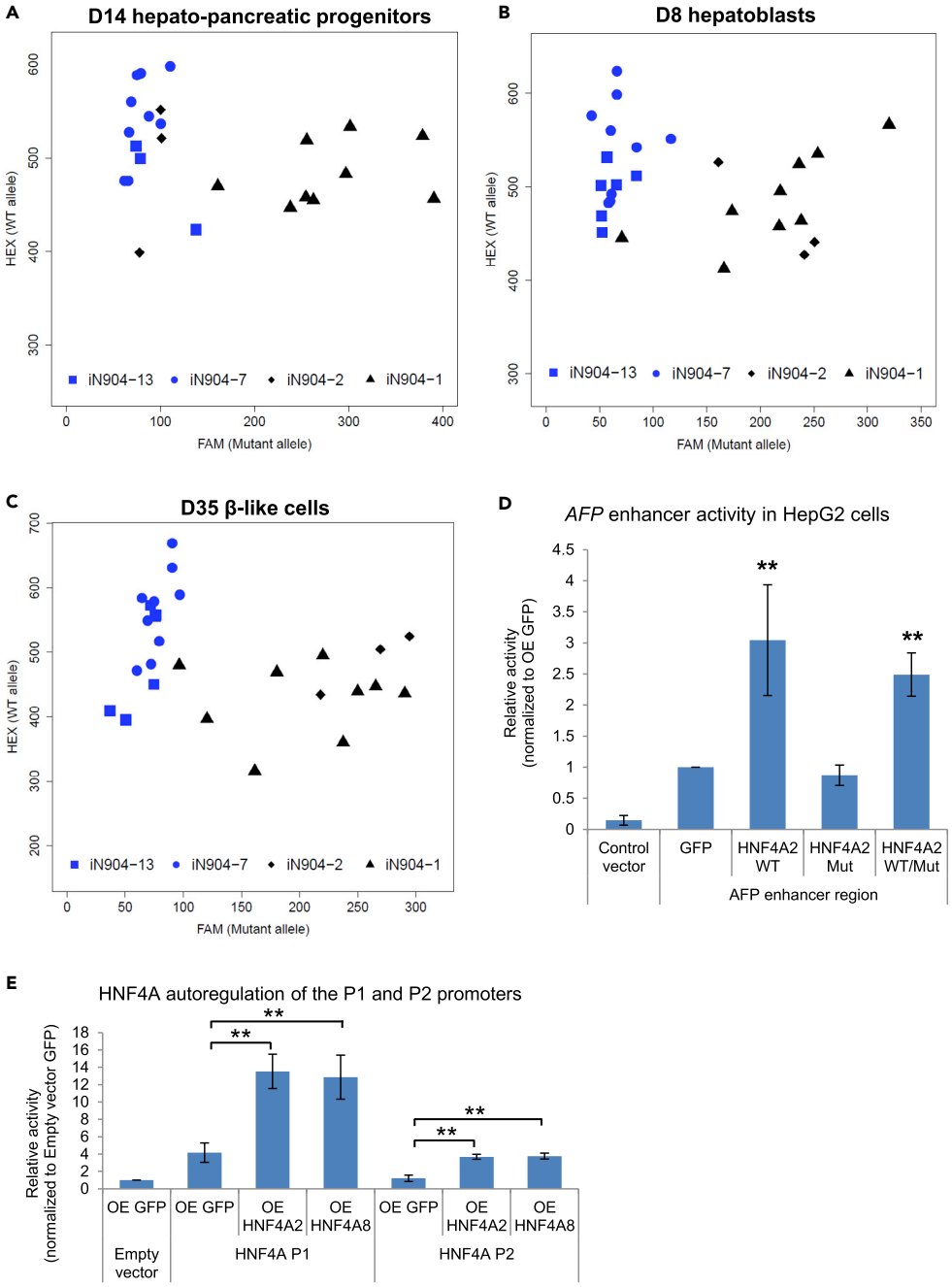

Figure 5. MODY1 hiPSC-Derived Cells Express Both WT and Mutant *HNF4A* Transcripts

(A–C) Allele-specific qPCR analyses in (A) D14 HPPs, (B) D8 hepatoblasts, and (C) D35 β-like cells evaluating both WT and mutant *HNF4A* transcripts in MODY1-derived cells. Axes show relative fluorescence units for each allele-specific TaqMan probe, for a representative differentiation experiment.

(D) Luciferase assays were performed to evaluate effects of WT and mutant HNF4A in combination with *AFP* enhancer activity in HepG2 cells.

(E) Luciferase assays were performed to evaluate effects of HNF4A2 and HNF4A8 on *HNF4A* P1 and P2 promoter activities in Ad293 cells.

Data are represented as mean ± SD of n = 4 independent experiments. **p < 0.01 versus GFP control unless otherwise indicated by Student's t test. See also Figure S5.

clinically significant given the lack of reports on liver deformities or severe liver dysfunction in these patients. Given the potential redundancy within the complex liver transcription factor network that HNF4A is involved in (Lau et al., 2018; Odom et al., 2004), there may be redundant mechanisms such as those involving HNF1A or ONECUT1 in the liver, or other compensatory mechanisms that enable largely normal liver development *in vivo* (Ober et al., 2006).

We also confirmed that although both P1- and P2-driven *HNF4A* are expressed during foregut differentiation, the primary isoform(s) that activates expression of key target genes such as *HNF1A* and *AFP* is likely encoded by the P1 promoter. These results are consistent with previous reports (Eeckhoute et al., 2003a) that P1-driven isoforms exhibit greater transcriptional potential than their P2-driven counterparts, and we show that this is the case in both human hepatic cells and β cells.

Besides a liver phenotype, patients with MODY1 are known to exhibit progressive β cell insulin secretory defects (Herman et al., 1997; Ryffel, 2001). Our studies provide valuable insights relating to the expression of early pancreatic genes affected by *HNF4A* haploinsufficiency such as *HNF1B*, *PDX1*, *GATA4,* and *RFX6* in the pancreatic progenitors. Although key developmental genes may be perturbed at the progenitor stage, the terminally *in vitro*-differentiated β-like cells were still able to express select β cell markers and C-peptide. This observation is in line with a previous study also involving MODY1-derived cells (Vethe et al., 2017). However, the study did not provide data from any of the progenitor stages. In both our study and that by Vethe et al., the *in vitro* differentiations do not generate β-like cells that are functionally mature despite the presence of insulin, therefore the functional capacity of these cells cannot be appropriately elucidated. As HNF4A haploinsufficiency involves a heterozygous mutation, there could be compensatory effects that result in a reset of the regulatory network, therefore patients do not have pancreatic agenesis. Nonetheless, there is a distinctive decrease in *HNF1A* expression in our MODY1-derived β-like cells. These findings are also consistent with the prevailing notion that MODY1/HNF4A is clinically and genetically linked to MODY3/HNF1A considering that HNF4A directly regulates the expression of *HNF1A* (Ellard and Colclough, 2006; Lausen et al., 2000). Detailed assessment of how the HNF4A-HNF1A cross-regulatory circuit and downstream transcriptional network is perturbed in both MODY1 and MODY3 may shed further light on the convergent and divergent role of both genes in governing tissue function, especially in human β cells.

It is notable that mutations in *HNF4A* are not only relevant to MODY1 but also have been associated with the more commonly occurring type 2 diabetes (T2D). Specifically, single nucleotide polymorphisms in both the P2 and P1 promoter regions and those near or within the *HNF4A* gene have been linked to T2D susceptibility (Damcott et al., 2004; Ek et al., 2005; Hara et al., 2006; Kooner et al., 2011; Love-Gregory et al., 2004; Mahajan et al., 2018; Silander et al., 2004; Weedon et al., 2004). Pancreatic islets isolated from donors with T2D were also found to exhibit reduced *HNF4A* expression (Gunton et al., 2005). Collectively, we report the successful establishment of a MODY1 hiPSC model with *HNF4A* haploinsufficiency that arose from a naturally occurring heterozygous mutation. Our findings highlight MODY1-*HNF4A* as a developmental disease that begins in the foregut endoderm and extends to its derivatives—in particular the liver and the pancreas. Our approach and results will have important implications for the study and understanding of diabetes pathogenesis in the context of MODY and even T2D.

Limitations of the Study

In this study, we have validated our findings across multiple differentiation models that can generate known cell-type-specific markers, as well as established mechanisms in non-iPSC-based cell lines to substantiate our findings of HNF4A haploinsufficiency. However, there are well-recognized limitations of iPSC-based disease models that can affect the interpretation of results. First, the differentiation process is heterogeneous and therefore a bulk analysis approach may result in data with overall increased variability and reduced magnitude of effect. To circumvent this, single-cell studies may be used to interrogate cellular phenotypes at single-cell resolution (Petersen et al., 2017). Second, the use of isogenic controls generated using genome-editing tools may also help to reduce noise when compared with the use of family controls, which are still subject to differences in genetic background (Teo et al., 2015a). Next, directed differentiation protocols rely on the use of a cocktail of small molecules and growth factors to drive the differentiation process *in vitro*. This assumes that patient cells encounter these signals under an *in vivo* setting to drive tissue development. Therefore, an *in vitro* model may not accurately capture disease progression. On the contrary, currently available pancreatic β cell differentiation protocols are often unable to generate functional

β cells *in vitro* and require transplantation into mice for *in vivo* maturation (Hrvatin et al., 2014; Loo et al., 2018). This hints at yet unknown molecular factors that are required to obtain β cells that can produce and secrete insulin in response to glucose stimuli. Therefore evaluation of the insulin secretory capacity of the MODY1-derived cells in the current differentiation model was not possible. Overcoming a number of these limitations will undoubtedly increase experimental robustness and reproducibility.

METHODS

All methods and can be found in the accompanying Transparent Methods supplemental file.

SUPPLEMENTAL INFORMATION

Supplemental Information can be found online at https://doi.org/10.1016/j.isci.2019.05.032.

ACKNOWLEDGMENTS

The authors thank Andreas Alvin Purnomo Soetedjo and Chek Mei Bok for experimental assistance and also thank members of the Teo laboratory for the critical reading of this manuscript. N.H.J.N. is supported by the National Medical Research Council (NMRC) Open Fund-Young Individual Research Grant (OF-YIRG) OFYIRG18May. R.N.K. acknowledges support from National Institutes of Health Grant RO1 067536. H.R. is supported by the Bergen Forskningsstiftelse (BFS), the Western Norway Regional Health Authority, the Novo Nordisk Foundation, and Diabetesforbundet. L.V. is funded by the ERC advanced grant New-Chol, the Cambridge University Hospitals National Institute for Health Research Biomedical Research Centre and the core support grant from the Wellcome Trust and Medical Research Council to the Wellcome–Medical Research Council Cambridge Stem Cell Institute. A.K.K.T. is supported by the Institute of Molecular and Cell Biology (IMCB), A*STAR, A*STAR JCO Career Development Award (CDA) 15302FG148, NMRC OFYIRG16may014, A*STAR ETPL Gap Funding ETPL/18-GAP005-R20H, Lee Foundation Grant SHTX/LFG/002/2018, Skin Innovation Grant SIG18011, NMRC OF-LCG/DYNAMO, FY2019 SingHealth Duke-NUS Surgery Academic Clinical Program Research Support Program Grant, and the Precision Medicine and Personalised Therapeutics Joint Research Grant 2019.

AUTHOR CONTRIBUTIONS

Conceptualization, A.K.K.T.; Methodology, N.H.J.N., J.B.J., and A.K.K.T.; Formal Analysis, N.H.J.N., J.B.J., and A.K.K.T.; Investigation, N.H.J.N., J.B.J., C.S.L., H.H.L., V.G.K., J.K., S.H., and A.K.K.T.; Resources, H.R., L.V., S.H., and A.K.K.T.; Writing – Original Draft, A.K.K.T.; Writing – Review & Editing, N.H.J.N., J.B.J., R.N.K., H.R., L.V., S.H., and A.K.K.T.; Visualization, N.H.J.N., J.B.J., and A.K.K.T.; Supervision, A.K.K.T.; Project Administration, A.K.K.T.; Funding Acquisition, A.K.K.T.

DECLARATION OF INTERESTS

The authors declare no competing interests.

Received: June 25, 2018
Revised: November 20, 2018
Accepted: May 22, 2019
Published: June 28, 2019

REFERENCES

Ameri, J., Stahlberg, A., Pedersen, J., Johansson, J.K., Johannesson, M.M., Artner, I., and Semb, H. (2010). FGF2 specifies hESC-derived definitive endoderm into foregut/midgut cell lineages in a concentration-dependent manner. Stem Cells *28*, 45–56.

Balbinot, C., Armant, O., Elarouci, N., Marisa, L., Martin, E., De Clara, E., Onea, A., Deschamps, J., Beck, F., Freund, J.N., et al. (2018). The Cdx2 homeobox gene suppresses intestinal tumorigenesis through non-cell-autonomous mechanisms. J. Exp. Med. *215*, 911–926.

Becker, H., Renner, S., Technau, G.M., and Berger, C. (2016). Cell-autonomous and non-cell-autonomous function of hox genes specify segmental neuroblast identity in the gnathal region of the embryonic CNS in Drosophila. PLoS Genet. *12*, e1005961.

Boj, S.F., Petrov, D., and Ferrer, J. (2010). Epistasis of transcriptomes reveals synergism between transcriptional activators Hnf1α and Hnf4α. PLoS Genet. *6*, e1000970.

Bolotin, E., Liao, H., Chi Ta, T., Yang, C., Hwang-Verslues, W., Evans, J.R., Jiang, T., and Sladek, F.M. (2010). Integrated approach for the identification of human hepatocyte nuclear factor 4α target genes using protein binding microarrays. Hepatology *51*, 642–653.

Byrne, M.M., Sturis, J., Fajans, S.S., Ortiz, F.J., Stoltz, A., Stoffel, M., Smith, M.J., Bell, G.I., Halter, J.B., and Polonsky, K.S. (1995). Altered insulin secretory responses to glucose in subjects with a mutation in the mody1 gene on chromosome-20. Diabetes *44*, 699–704.

Damcott, C.M., Hoppman, N., Ott, S.H., Reinhart, L.J., Wang, J., Pollin, T.I., O'Connell, J.R.,

Mitchell, B.D., and Shuldiner, A.R. (2004). Polymorphisms in both promoters of hepatocyte nuclear factor 4-alpha are associated with type 2 diabetes in the Amish. Diabetes *53*, 3337–3341.

DeLaForest, A., Nagaoka, M., Si-Tayeb, K., Noto, F.K., Konopka, G., Battle, M.A., and Duncan, S.A. (2011). HNF4A is essential for specification of hepatic progenitors from human pluripotent stem cells. Development *138*, 4143–4153.

Eeckhoute, J., Moerman, E., Bouckenooghe, T., Lukoviak, B., Pattou, F., Formstecher, P., Kerr-Conte, J., Vandewalle, B., and Laine, B. (2003a). Hepatocyte nuclear factor 4 alpha isoforms originated from the P1 promoter are expressed in human pancreatic beta-cells and exhibit stronger transcriptional potentials than P2 promoter-driven isoforms. Endocrinology *144*, 1686–1694.

Eeckhoute, J., Oxombre, B., Formstecher, P., Lefebvre, P., and Laine, B. (2003b). Critical role of charged residues in helix 7 of the ligand binding domain in Hepatocyte Nuclear Factor 4α dimerisation and transcriptional activity. Nucleic Acids Res. *31*, 6640–6650.

Ek, J., Rose, C.S., Jensen, D.P., Glumer, C., Borch-Johnsen, K., Jorgensen, T., Pedersen, O., and Hansen, T. (2005). The functional Thr130Ile and Val255Met polymorphisms of the hepatocyte nuclear factor-4 alpha (HNF4A): gene associations with type 2 diabetes or altered beta-cell function among Danes. J. Clin. Endocrinol. Metab. *90*, 3054–3059.

Ellard, S., and Colclough, K. (2006). Mutations in the genes encoding the transcription factors hepatocyte nuclear factor 1 alpha (HNF1A) and 4 alpha (HNF4A) in maturity-onset diabetes of the young. Hum. Mutat. *27*, 854–869.

Frischmeyer, P.A., and Dietz, H.C. (1999). Nonsense-mediated mRNA decay in health and disease. Hum. Mol. Genet. *8*, 1893–1900.

Gardner, D.S.L., and Tai, E.S. (2012). Clinical features and treatment of maturity onset diabetes of the young (MODY). Diabetes Metab. Syndr. Obes. *5*, 101–108.

Gunton, J.E., Kulkarni, R.N., Yim, S., Okada, T., Hawthorne, W.J., Tseng, Y.-H., Roberson, R.S., Ricordi, C., O'Connell, P.J., Gonzalez, F.J., et al. (2005). Loss of ARNT/HIF1β mediates altered gene expression and pancreatic-islet dysfunction in human type 2 diabetes. Cell *122*, 337–349.

Gupta, R.K., Vatamaniuk, M.Z., Lee, C.S., Flaschen, R.C., Fulmer, J.T., Matschinsky, F.M., Duncan, S.A., and Kaestner, K.H. (2005). The MODY1 gene HNF-4α regulates selected genes involved in insulin secretion. J. Clin. Invest. *115*, 1006–1015.

Hani, E., Suaud, L., Boutin, P., Chevre, J.C., Durand, E., Philippi, A., Demenais, F., Vionnet, N., Furuta, H., Velho, G., et al. (1998). A missense mutation in hepatocyte nuclear factor-4 alpha, resulting in a reduced transactivation activity, in human late-onset non-insulin-dependent diabetes mellitus. J. Clin. Invest. *101*, 521–526.

Hannan, N.R., Segeritz, C.P., Touboul, T., and Vallier, L. (2013). Production of hepatocyte-like cells from human pluripotent stem cells. Nat. Protoc. *8*, 430–437.

Hara, K., Horikoshi, M., Kitazato, H., Lto, C., Noda, M., Ohashi, J., Froguel, P., Tokunaga, K., Tobe, K., Nagai, R., et al. (2006). Hepatocyte nuclear factor-4 alpha P2 promoter haplotypes are associated with type 2 diabetes in the Japanese population. Diabetes *55*, 1260–1264.

Harries, L.W., Locke, J.M., Shields, B., Hanley, N.A., Hanley, K.P., Steele, A., Njolstad, P.R., Ellard, S., and Hattersley, A.T. (2008). The diabetic phenotype in HNF4A mutation carriers is moderated by the expression of HNF4A isoforms from the P1 promoter during fetal development. Diabetes *57*, 1745–1752.

Herman, W.H., Fajans, S.S., Smith, M.J., Polonsky, K.S., Bell, G.I., and Halter, J.B. (1997). Diminished insulin and glucagon secretory responses to arginine in nondiabetic subjects with a mutation in the hepatocyte nuclear factor-4alpha/MODY1 gene. Diabetes *46*, 1749–1754.

Hrvatin, S., O'Donnell, C.W., Deng, F., Millman, J.R., Pagliuca, F.W., Dilorio, P., Rezania, A., Gifford, D.K., and Melton, D.A. (2014). Differentiated human stem cells resemble fetal, not adult, beta cells. Proc. Natl. Acad. Sci. U S A *111*, 3038–3043.

Huang, J., Levitsky, L.L., and Rhoads, D.B. (2009). Novel P2 promoter-derived HNF4α isoforms with different N-terminus generated by alternate exon insertion. Exp. Cell Res. *315*, 1200–1211.

Jiang, S., Tanaka, T., Iwanari, H., Hotta, H., Yamashita, H., Kumakura, J., Watanabe, Y., Uchiyama, Y., Aburatani, H., Hamakubo, T., et al. (2003). Expression and localization of P1 promoter-driven hepatocyte nuclear factor-4α (HNF4α) isoforms in human and rats. Nucl. Recept. *1*, 1–12.

Kawai, H.F., Kaneko, S., Honda, M., Shirota, Y., and Kobayashi, K. (2001). alpha-fetoprotein-producing hepatoma cell lines share common expression profiles of genes in various categories demonstrated by cDNA microarray analysis. Hepatology *33*, 676–691.

Kooner, J.S., Saleheen, D., Sim, X., Sehmi, J., Zhang, W., Frossard, P., Been, L.F., Chia, K.S., Dimas, A.S., Hassanali, N., et al. (2011). Genome-wide association study in individuals of South Asian ancestry identifies six new type 2 diabetes susceptibility loci. Nat. Genet. *43*, 984–989.

Laine, B., Eeckhoute, J., Suaud, L., Briche, I., Furuta, H., Bell, G.I., and Formstecher, P. (2000). Functional properties of the R154X HNF-4alpha protein generated by a mutation associated with maturity-onset diabetes of the young, type 1. FEBS Lett. *479*, 41–45.

Lau, H.H., Ng, N.H.J., Loo, L.S.W., Jasmen, J.B., and Teo, A.K.K. (2018). The molecular functions of hepatocyte nuclear factors - in and beyond the liver. J. Hepatol. *68*, 1033–1048.

Lausen, J., Thomas, H., Lemm, I., Bulman, M., Borgschulze, M., Lingott, A., Hattersley, A.T., and Ryffel, G.U. (2000). Naturally occurring mutations in the human HNF4alpha gene impair the function of the transcription factor to a varying degree. Nucleic Acids Res. *28*, 430–437.

Lehto, M., Bitzen, P.O., Isomaa, B., Wipemo, C., Wessman, Y., Forsblom, C., Tuomi, T., Taskinen, M.R., and Groop, L. (1999). Mutation in the HNF-4alpha gene affects insulin secretion and triglyceride metabolism. Diabetes *48*, 423–425.

Li, J., Ning, G., and Duncan, S.A. (2000). Mammalian hepatocyte differentiation requires the transcription factor HNF-4α. Genes Dev. *14*, 464–474.

Loo, L.S.W., Lau, H.H., Jasmen, J.B., Lim, C.S., and Teo, A.K.K. (2018). An arduous journey from human pluripotent stem cells to functional pancreatic beta cells. Diabetes Obes. Metab. *20*, 3–13.

Love-Gregory, L.D., Wasson, J., Ma, J., Jin, C.H., Glaser, B., Suarez, B.K., and Permutt, M.A. (2004). A common polymorphism in the upstream promoter region of the hepatocyte nuclear factor-4 alpha gene on chromosome 20q is associated with type 2 diabetes and appears to contribute to the evidence for linkage in an ashkenazi jewish population. Diabetes *53*, 1134–1140.

Mahajan, A., Wessel, J., Willems, S.M., Zhao, W., Robertson, N.R., Chu, A.Y., Gan, W., Kitajima, H., Taliun, D., Rayner, N.W., et al. (2018). Refining the accuracy of validated target identification through coding variant fine-mapping in type 2 diabetes. Nat. Genet. *50*, 559–571.

Miura, A., Yamagata, K., Kakei, M., Hatakeyama, H., Takahashi, N., Fukui, K., Nammo, T., Yoneda, K., Inoue, Y., Sladek, F.M., et al. (2006). Hepatocyte nuclear factor-4alpha is essential for glucose-stimulated insulin secretion by pancreatic beta-cells. J. Biol. Chem. *281*, 5246–5257.

Nakabayashi, H., Koyama, Y., Suzuki, H., Li, H.M., Sakai, M., Miura, Y., Wong, N.C., and Nishi, S. (2004). Functional mapping of tissue-specific elements of the human alpha-fetoprotein gene enhancer. Biochem. Biophys. Res. Commun. *318*, 773–785.

Nammo, T., Yamagata, K., Tanaka, T., Kodama, T., Sladek, F.M., Fukui, K., Katsube, F., Sato, Y., Miyagawa, J., and Shimomura, I. (2008). Expression of HNF-4alpha (MODY1), HNF-1beta (MODY5), and HNF-1alpha (MODY3) proteins in the developing mouse pancreas. Gene Expr. Patterns *8*, 96–106.

Ober, E.A., Verkade, H., Field, H.A., and Stainier, D.Y. (2006). Mesodermal Wnt2b signalling positively regulates liver specification. Nature *442*, 688–691.

Odom, D.T., Zizlsperger, N., Gordon, D.B., Bell, G.W., Rinaldi, N.J., Murray, H.L., Volkert, T.L., Schreiber, J., Rolfe, P.A., Gifford, D.K., et al. (2004). Control of pancreas and liver gene expression by HNF transcription factors. Science *303*, 1378–1381.

Pagliuca, F.W., Millman, J.R., Gurtler, M., Segel, M., Van Dervort, A., Ryu, J.H., Peterson, Q.P., Greiner, D., and Melton, D.A. (2014). Generation of functional human pancreatic beta cells in vitro. Cell *159*, 428–439.

Pearson, E.R., Pruhova, S., Tack, C.J., Johansen, A., Castleden, H.A.J., Lumb, P.J., Wierzbicki, A.S., Clark, P.M., Lebl, J., Pedersen, O., et al. (2005). Molecular genetics and phenotypic characteristics of MODY caused by hepatocyte nuclear factor 4α mutations in a large European collection. Diabetologia *48*, 878–885.

Petersen, M.B.K., Azad, A., Ingvorsen, C., Hess, K., Hansson, M., Grapin-Botton, A., and Honore, C. (2017). Single-cell gene expression analysis of a human ESC model of pancreatic endocrine development reveals different paths to beta-cell differentiation. Stem Cell Reports *9*, 1246–1261.

Ryffel, G.U. (2001). Mutations in the human genes encoding the transcription factors of the hepatocyte nuclear factor (HNF)1 and HNF4 families: functional and pathological consequences. J. Mol. Endocrinol. *27*, 11–29.

Shih, D.Q., Dansky, H.M., Fleisher, M., Assmann, G., Fajans, S.S., and Stoffel, M. (2000). Genotype/phenotype relationships in HNF-4alpha/MODY1: haploinsufficiency is associated with reduced apolipoprotein (AII), apolipoprotein (CIII), lipoprotein(a), and triglyceride levels. Diabetes *49*, 832–837.

Silander, K., Mohlke, K.L., Scott, L.J., Peck, E.C., Hollstein, P., Skol, A.D., Jackson, A.U., Deloukas, P., Hunt, S., Stavrides, G., et al. (2004). Genetic variation near the hepatocyte nuclear factor-4 alpha gene predicts susceptibility to type 2 diabetes. Diabetes *53*, 1141–1149.

Sladek, F.M., Dallas-Yang, Q., and Nepomuceno, L. (1998). MODY1 mutation Q268X in hepatocyte nuclear factor 4alpha allows for dimerization in solution but causes abnormal subcellular localization. Diabetes *47*, 985–990.

Sladek, F.M., Zhong, W.M., Lai, E., and Darnell, J.E., Jr. (1990). Liver-enriched transcription factor HNF-4 is a novel member of the steroid hormone receptor superfamily. Genes Dev. *4*, 2353–2365.

Stoffel, M., and Duncan, S.A. (1997). The maturity-onset diabetes of the young (MODY1) transcription factor HNF4 alpha regulates expression of genes required for glucose transport and metabolism. Proc. Natl. Acad. Sci. U S A *94*, 13209–13214.

Tanaka, T., Jiang, S., Hotta, H., Takano, K., Iwanari, H., Sumi, K., Daigo, K., Ohashi, R., Sugai, M., Ikegame, C., et al. (2006). Dysregulated expression of P1 and P2 promoter-driven hepatocyte nuclear factor-4α in the pathogenesis of human cancer. J. Pathol. *208*, 662–672.

Teo, A.K., Gupta, M.K., Doria, A., and Kulkarni, R.N. (2015a). Dissecting diabetes/metabolic disease mechanisms using pluripotent stem cells and genome editing tools. Mol. Metab. *4*, 593–604.

Teo, A.K., Lau, H.H., Valdez, I.A., Dirice, E., Tjora, E., Raeder, H., and Kulkarni, R.N. (2016). Early developmental perturbations in a human stem cell model of MODY5/HNF1B pancreatic hypoplasia. Stem Cell Reports *6*, 357–367.

Teo, A.K., Tsuneyoshi, N., Hoon, S., Tan, E.K., Stanton, L.W., Wright, C.V., and Dunn, N.R. (2015b). PDX1 binds and represses hepatic genes to ensure robust pancreatic commitment in differentiating human embryonic stem cells. Stem Cell Reports *4*, 578–590.

Teo, A.K., Wagers, A.J., and Kulkarni, R.N. (2013a). New opportunities: harnessing induced pluripotency for discovery in diabetes and metabolism. Cell Metab. *18*, 775–791.

Teo, A.K., Windmueller, R., Johansson, B.B., Dirice, E., Njolstad, P.R., Tjora, E., Raeder, H., and Kulkarni, R.N. (2013b). Derivation of human induced pluripotent stem cells from patients with maturity onset diabetes of the young. J. Biol. Chem. *288*, 5353–5356.

Vethe, H., Bjorlykke, Y., Ghila, L.M., Paulo, J.A., Scholz, H., Gygi, S.P., Chera, S., and Raeder, H. (2017). Probing the missing mature beta-cell proteomic landscape in differentiating patient iPSC-derived cells. Sci. Rep. *7*, 4780.

Weedon, M.N., Owen, K.R., Shields, B., Hitman, G., Walker, M., McCarthy, M.I., Love-Gregory, L.D., Permutt, M.A., Hattersley, A.T., and Frayling, T.M. (2004). Common variants of the hepatocyte nuclear factor-4 alpha P2 promoter are associated with type 2 diabetes in the UK population. Diabetes *53*, 3002–3006.

Yamagata, K., Furuta, H., Oda, N., Kaisaki, P.J., Menzel, S., Cox, N.J., Fajans, S.S., Signorini, S., Stoffel, M., and Bell, G.I. (1996). Mutations in the hepatocyte nuclear factor-4[alpha] gene in maturity-onset diabetes of the young (MODY1). Nature *384*, 458–460.

Zhang, Z., Xin, D., Wang, P., Zhou, L., Hu, L., Kong, X., and Hurst, L.D. (2009). Noisy splicing, more than expression regulation, explains why some exons are subject to nonsense-mediated mRNA decay. BMC Biol. *7*, 23.

ISCI, Volume *16*

Supplemental Information

HNF4A Haploinsufficiency in MODY1 Abrogates Liver and Pancreas Differentiation from Patient-Derived Induced Pluripotent Stem Cells

Natasha Hui Jin Ng, Joanita Binte Jasmen, Chang Siang Lim, Hwee Hui Lau, Vidhya Gomathi Krishnan, Juned Kadiwala, Rohit N. Kulkarni, Helge Ræder, Ludovic Vallier, Shawn Hoon, and Adrian Kee Keong Teo

Supplemental Figure S1: Ng et al.

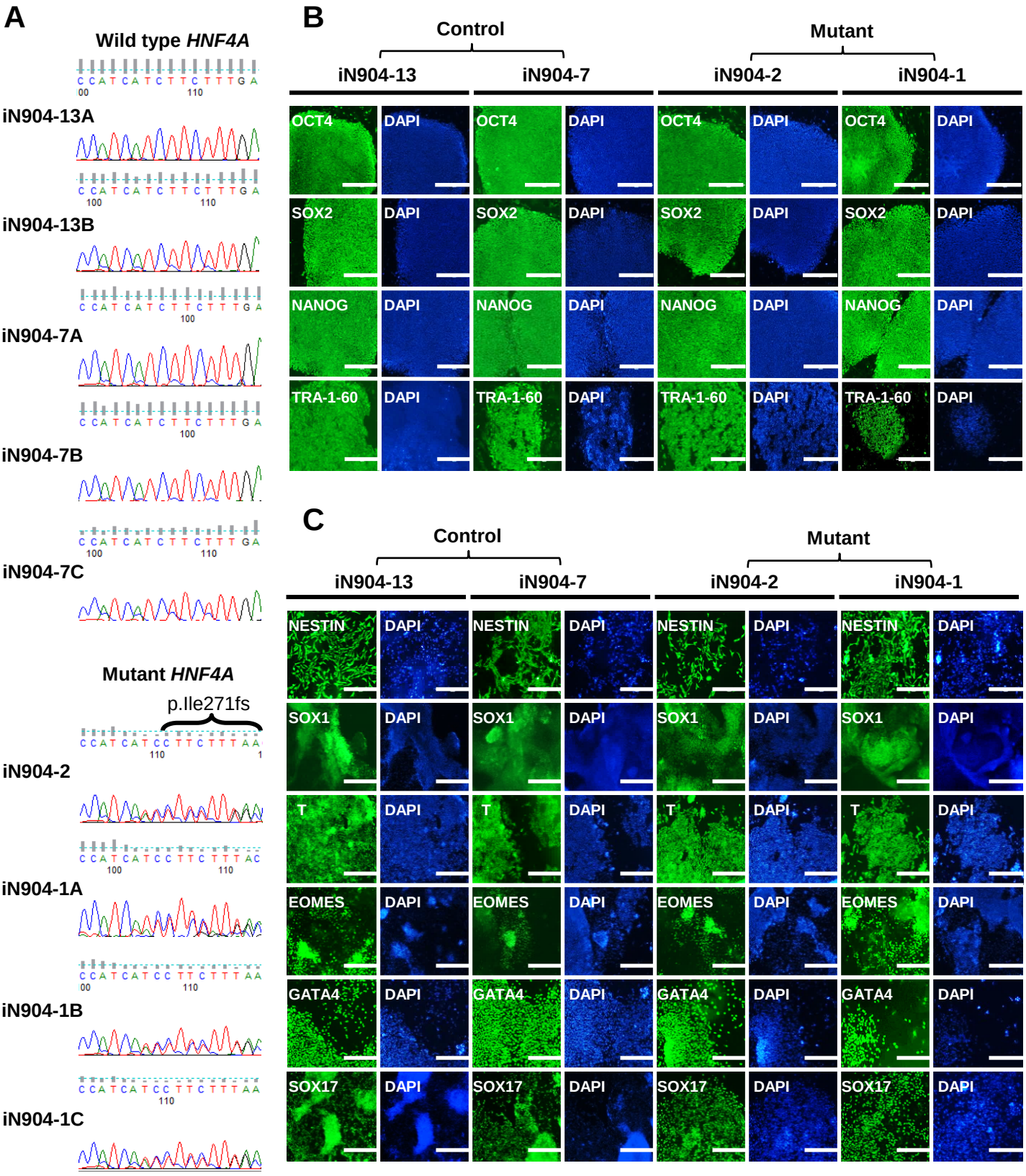

Figure S1, related to Figure 1. Characterization of MODY1-hiPSCs. (**A**) DNA sequencing to verify absence or presence of *HNF4A* p.Ile271fs mutation in control- and MODY1-hiPSCs. Control- and MODY1-hiPSCs (**B**) express pluripotency markers and (**C**) can give rise to cell types making up the three germ layers. Scale bars: 400 µm.

Supplemental Figure S2: Ng et al.

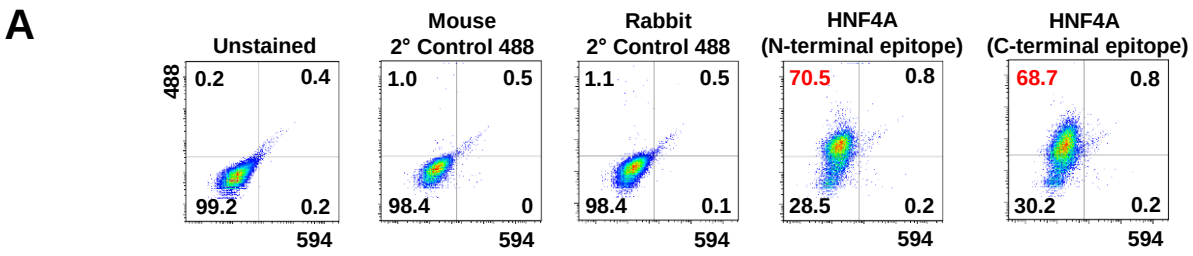

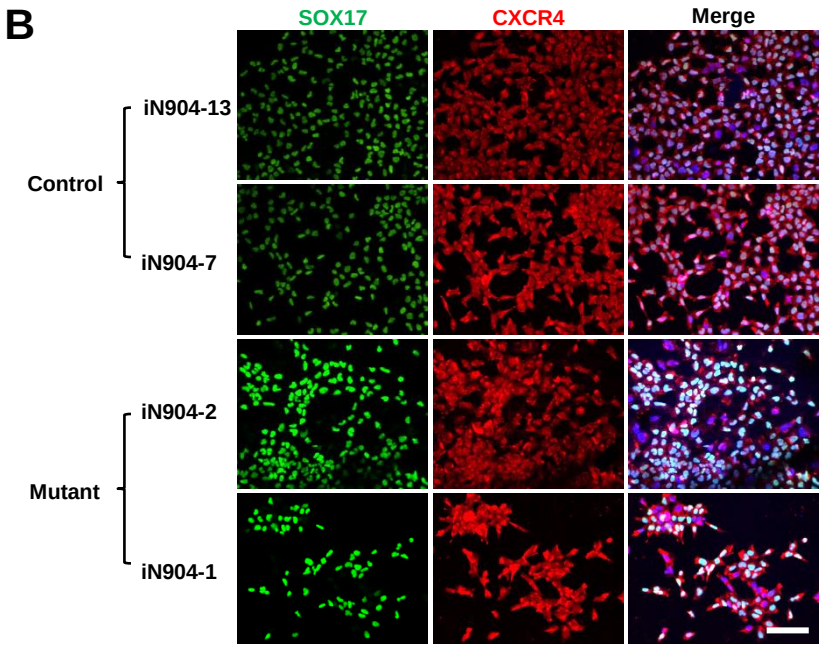

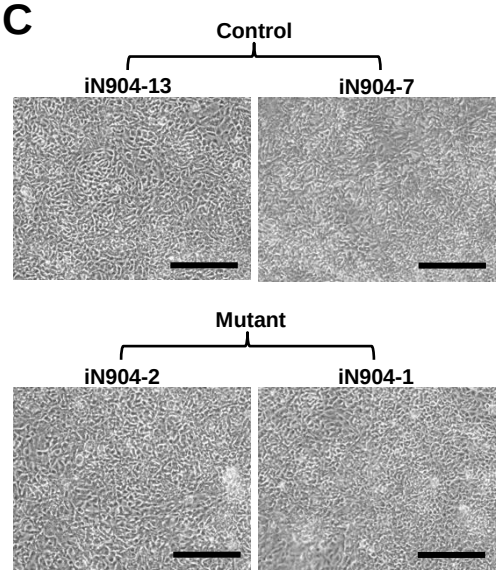

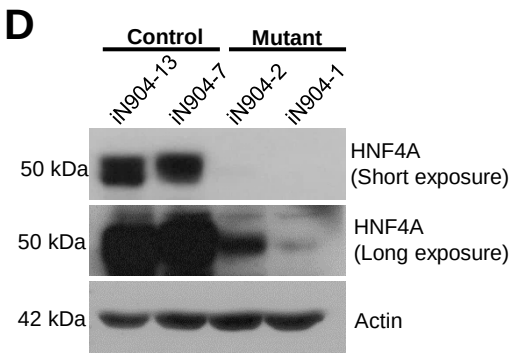

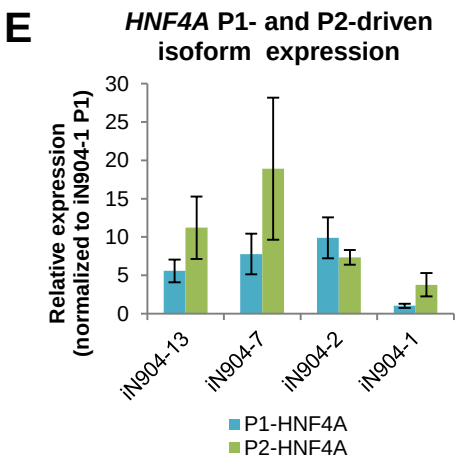

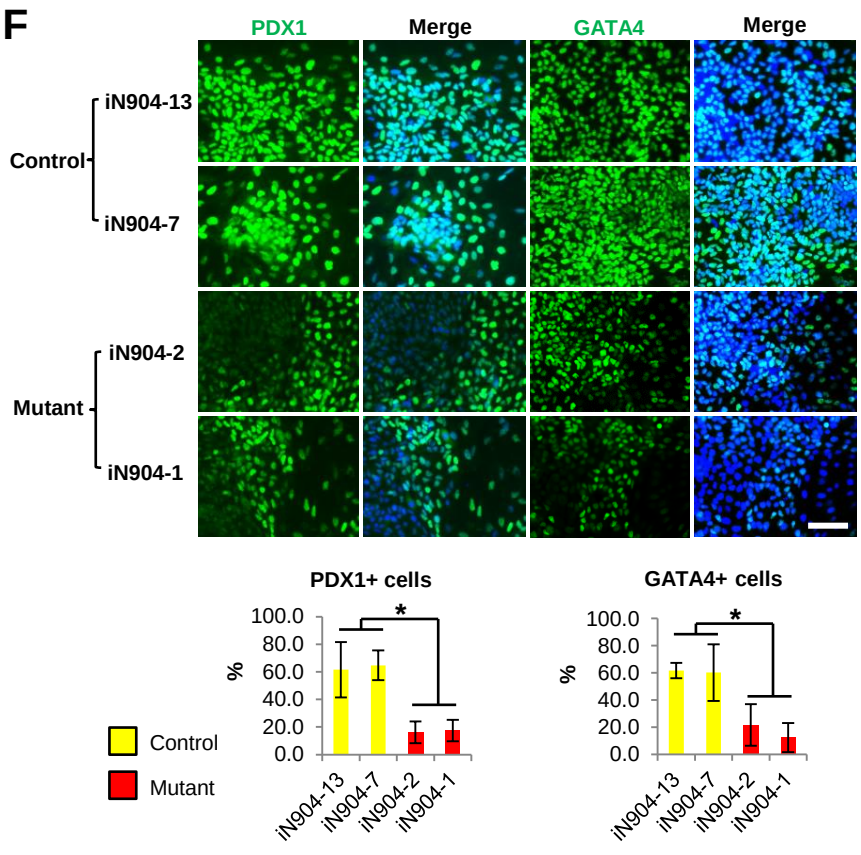

Figure S2, related to Figure 2. Characterization of the differentiation of iPSCs into D14 HPPs.

(**A**) ~70% of control-hPSC-derived cells are HNF4A^{+} based on FACS analysis. (**B**) Co-expression of definitive endoderm markers SOX17 (Green, R&D AF1924) and CXCR4 (Red, BD 555976) was determined at day 3 of differentiation. (**C**) No obvious morphological differences were observed between control- and MODY1-HPPs after 14 days of differentiation. (**D**) Western blot analysis using an antibody against the HNF4A C-terminal epitope (that recognizes full-length but not C-terminally-truncated protein) shows markedly reduced levels of HNF4A WT protein in MODY1-HPPs. (**E**) Both *HNF4A* P1 and P2 promoter-driven transcripts are expressed by isoform-specific qPCR analysis. Data are represented as mean ± SD of n=3, representative of 3 independent experiments. (**F**) Expression of pancreatic progenitor markers PDX1 (R&D AF2419) and GATA4 (Thermo Fisher 6H10) was downregulated in MODY1-HPPs compared to controls. The percentage of PDX1- or GATA4-positive cells were quantified from at least 3 different images, each with 189-594 cells counted. Data are represented as mean ± SD of n=3. *$p < 0.05$ versus controls as indicated by Student's t test. Scale bars: 100 μm.

Supplemental Figure S3: Ng et al.

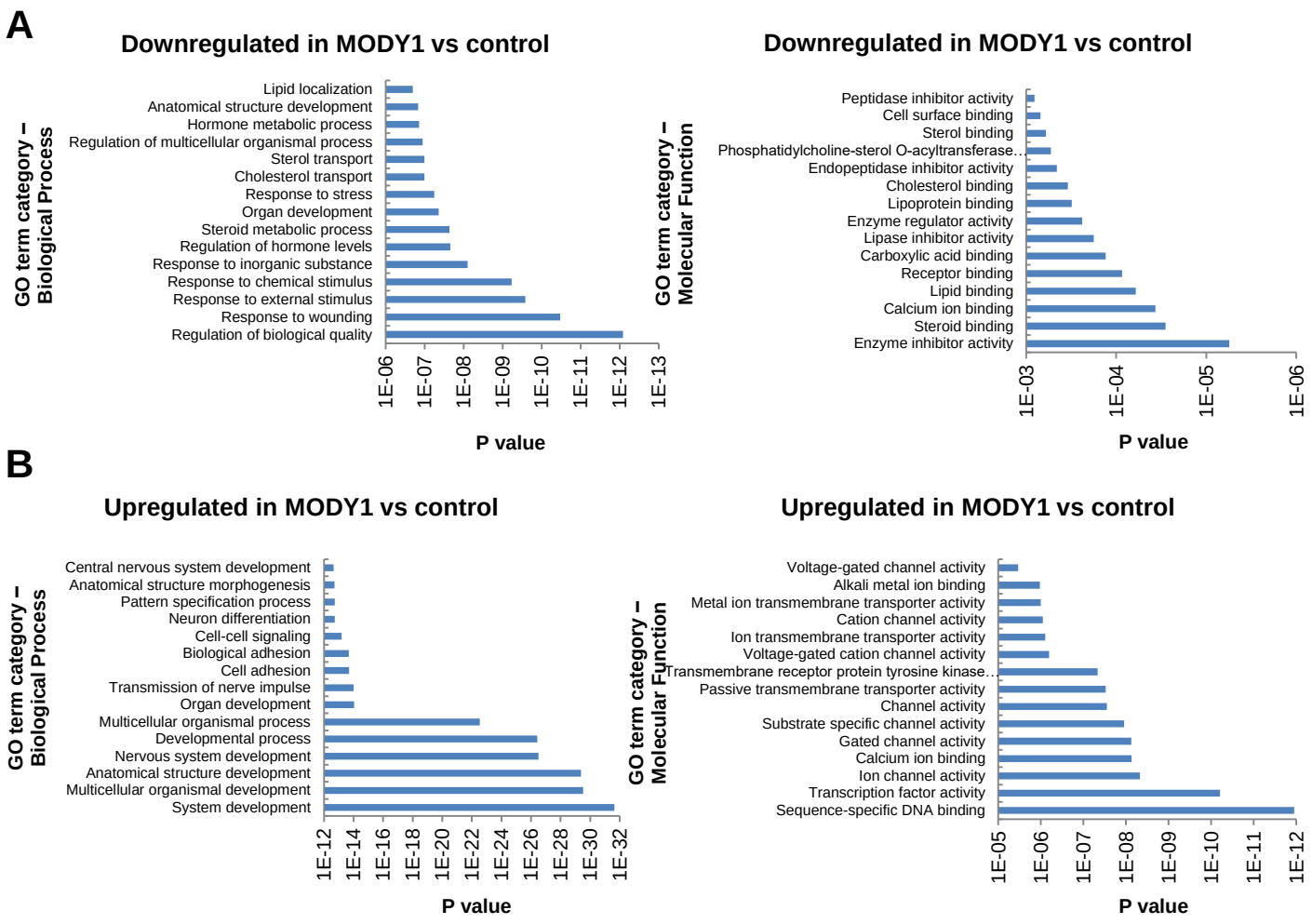

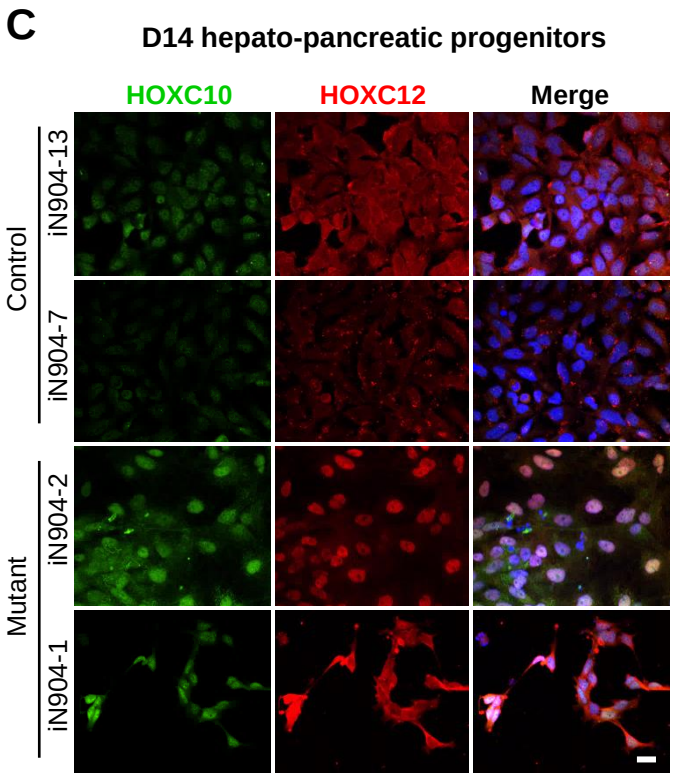

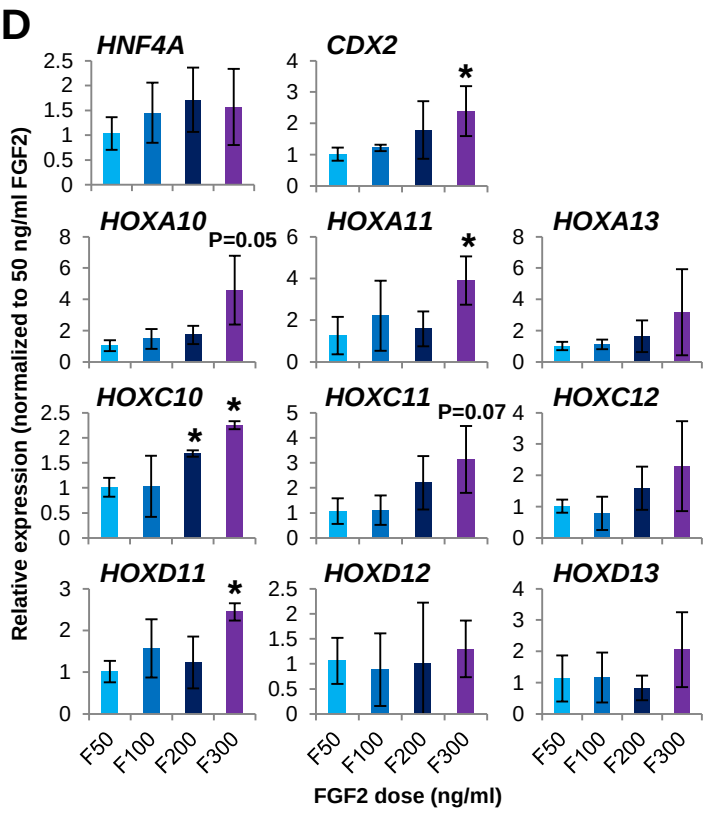

Figure S3, related to Figure 2 and Table S1. Gene ontology analyses of global transcriptional changes induced by the *HNF4A* (p.Ile271fs) mutation in MODY1-HPPs.

(**A**) Downregulated genes were involved in biological processes related to steroid metabolism and sterol transport, and molecular functions related to enzyme inhibitor activity, lipoprotein and sterol binding. (**B**) Upregulated genes were important for developmental processes and molecular functions related to DNA binding and channel activity. (**C**) Expression of representative hindgut markers HOXC10 and HOXC12 were evaluated by immunofluorescent confocal microscopy in D14 HPPs. Blue: DAPI, Green: HOXC10, Red: HOXC12. Scale bar: 50 µm. (**D**) High dose of FGF2 treatment increases the expression of caudal *HOX* genes. Data are represented as mean ± SD of n=3, representative of 3 independent experiments. *P<0.05 versus 50 ng/ml FGF2 (F50) samples by Student's *t*-test.

Supplemental Figure S4: Ng et al.

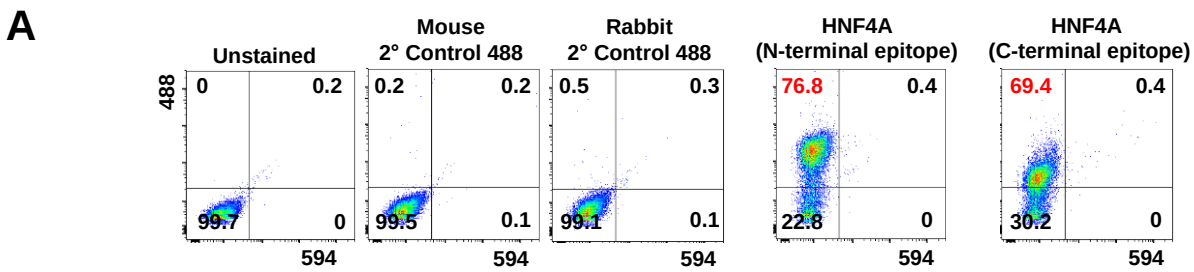

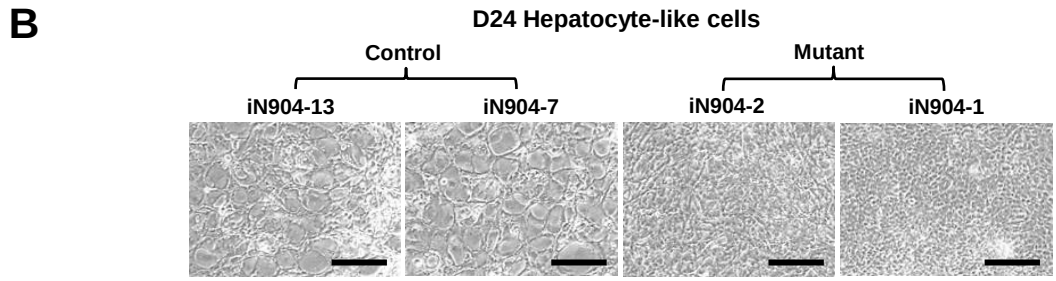

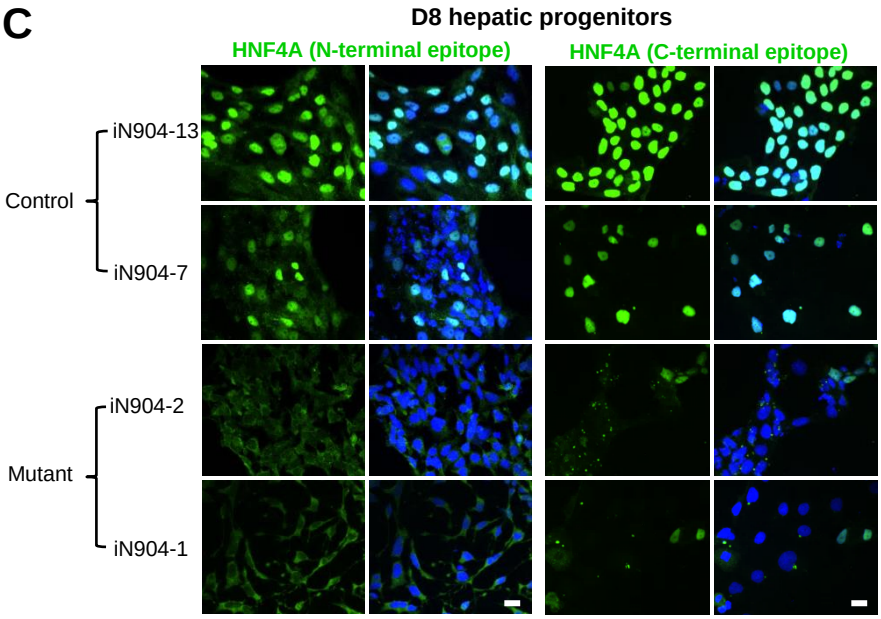

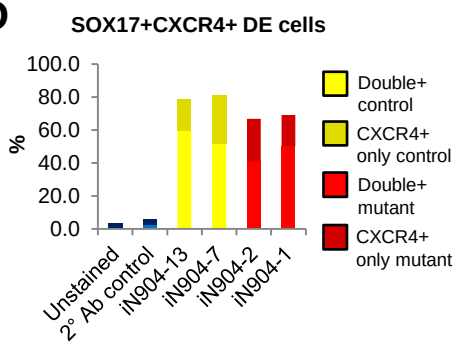

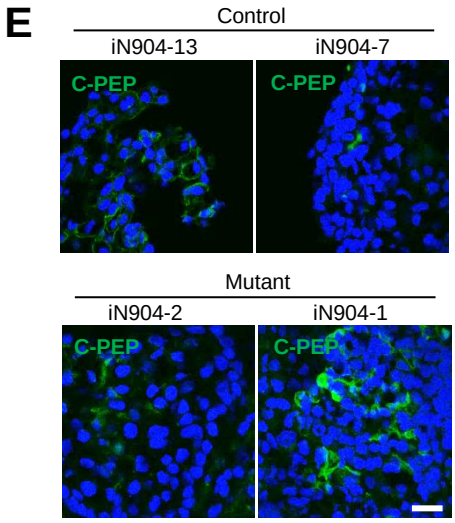

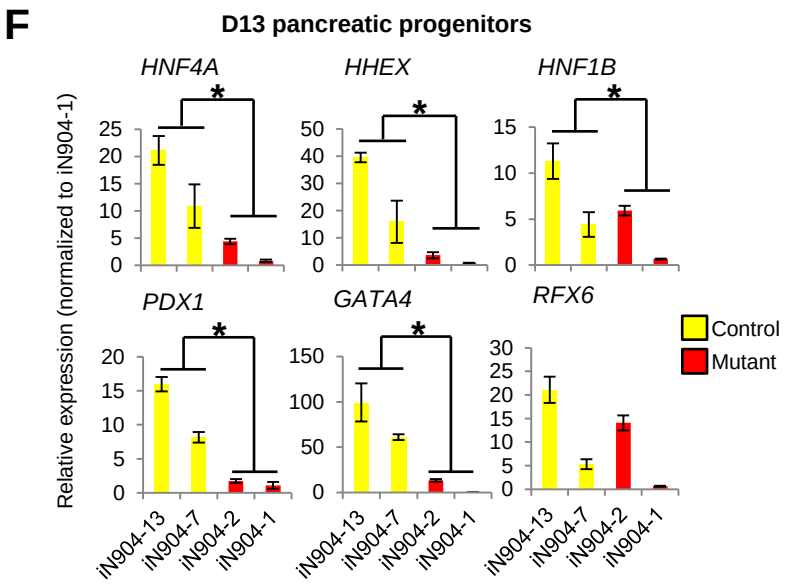

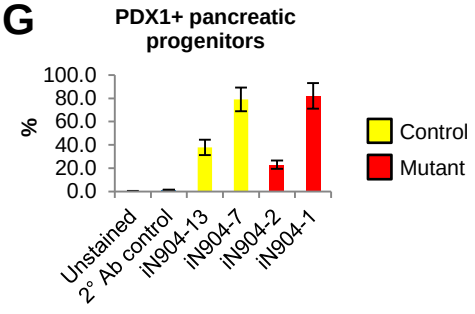

Figure S4, related to Figure 3. Characterization of hiPSC-derived hepatic and pancreatic cells.

(**A**) FACS analysis using HNF4A antibodies targeting the N- or C-terminal regions showing that 70 – 80% of control-hPSC-derived hepatic progenitors are HNF4A^{+} at D8. (**B**) Brightfield images showing that hepatocyte-like cells derived from MODY1-hiPSCs lack a polygonal morphology after 24 days of differentiation. Scale bar: 100 µm. (**C**) Immunofluorescent confocal images showing that HNF4A protein is predominantly localized to the nuclei in control D8 hepatic progenitors but is largely sequestered in the cytoplasm of MODY1 hepatic progenitors, based on antibodies targeting the N- or C-terminal regions of HNF4A. Blue: DAPI, Green: HNF4A, Scale bars: 50 µm. Confocal images were acquired using similar scan settings across samples. (**D**) FACS analysis showed co-expression of definitive endoderm (DE) markers SOX17-PE (R&D IC19241P) and CXCR4-APC (BD 555976) indicated as 'double+', and expression of CXCR4 alone ('CXCR4+ only') in control- and MODY1-derived cells after 5 days of differentiation in suspension cultures, using the β cell differentiation protocol adapted from Pagliuca et al. Data obtained from one experiment. (**E**) Immunofluorescence staining revealed expression of C-peptide (Green, DSHB GN-ID4) in both control- and MODY1-derived day 35 β-like cells. Blue: DAPI; scale bar: 50 µm. (**F**) QPCR analyses of D13 pancreatic progenitors generated using the β cell differentiation protocol were used to compare gene expression changes between control- and MODY1-derived cells. Data are represented as mean ± SD of n=3, representative of up to 3 independent experiments. *P<0.05 vs controls by Student's *t*-test. (**G**) FACS analysis showed expression of PDX1 (Abcam ab47308) in Day 13 pancreatic progenitors obtained using the β cell differentiation protocol. Data are represented as mean ± SD of n=2 independent experiments.

Supplemental Figure S5: Ng et al.

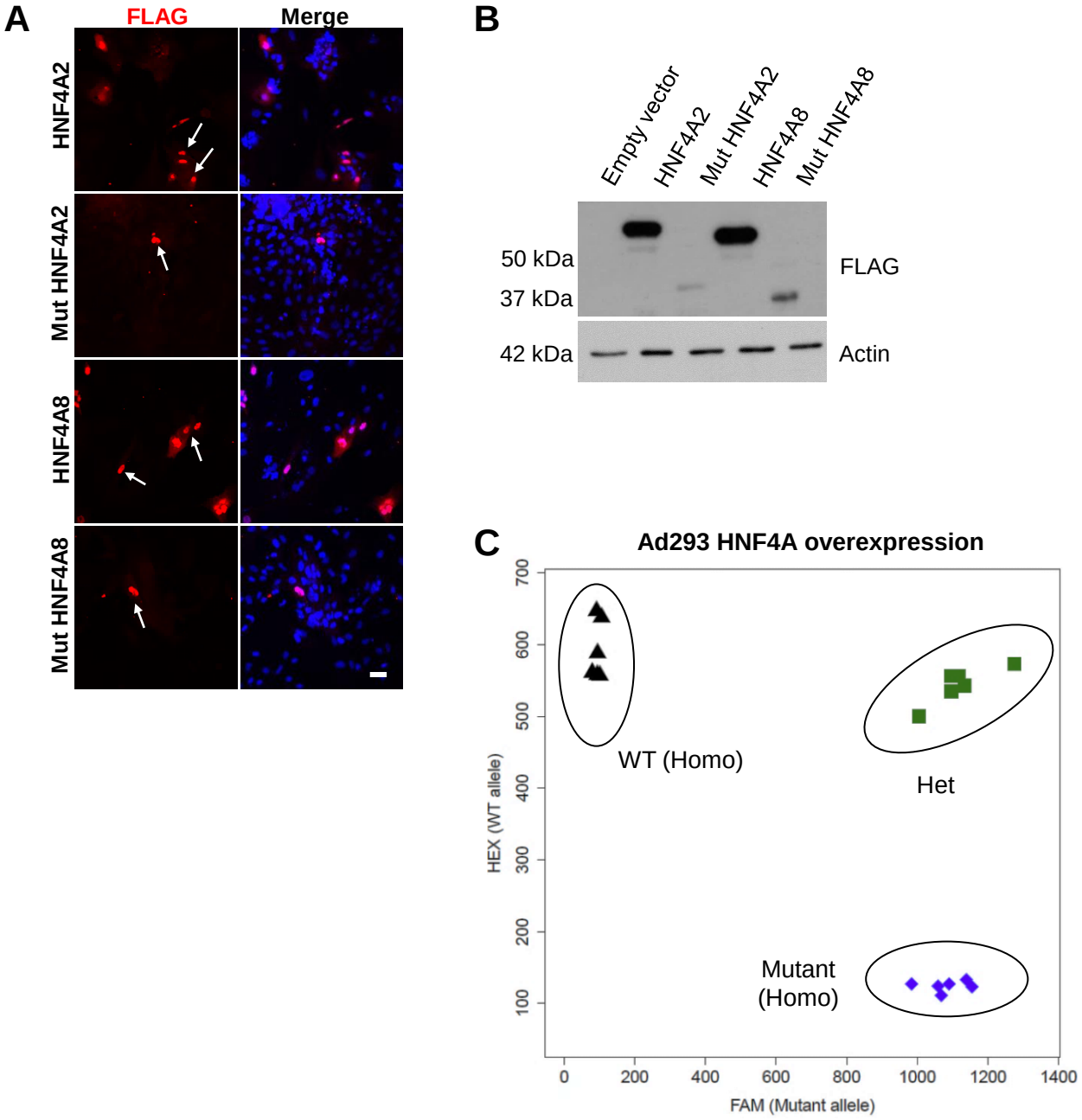

Figure S5, related to Figures 4 and 5. Validation of HNF4A WT and mutant overexpression.

Transient overexpression of WT and mutant (Mut) HNF4A2 and HNF4A8 constructs (N-terminal FLAG-tagged) are validated by (**A**) immunostaining in hiPSC-derived D16 hepatic progenitors and (**B**) western blot analysis in Ad293 cells. Blue: DAPI, Red: FLAG-tagged HNF4A, Scale bar: 50 µm. (**C**) Allele-specific qPCR analyses of mRNA from Ad293 transfected with HNF4A2 or HNF4A8 WT and/or mutant constructs, in triplicates, showed clear segregation among the genotypes. Axes show relative fluorescence units for each allele-specific TaqMan probe.

Table S1 (Excel table, related to Figures 2 and S3). Expression values (RPKM) of hiPSC-derived HPPs at D14 from RNA-Seq data. The first 2 columns indicate the gene ID and official gene symbol for all protein-coding genes in the dataset. FPKM values are shown for control-hiPSC-derived cells (13A, 13B, 7A, 7B, 7C) and MODY1-hiPSC-derived cells (2, 1A, 1B, 1C).

Table S2 (Related to Methods, Figures 1, 2 and 3). Quantitative real-time PCR primers used in this study.

Gene	Accession Number	Forward Primer (5' to 3')	Reverse Primer (5' to 3')
ABCC8	NM_001287174.1	GGAGCAGCAGCCTTCCTGACA	TGCGAAGCATAGGCCACGGG
ACTIN	NM_001101.3	TTGCCGATCCGCCGCCCGTC	CCCATGCCCACCATCACGCCCTGG
AFP	NM_001134.2	TGCTTCCAAACAAAGGCAGCAACAG	TGTACATGGGCCACATCCAGGAC
ALB	NM_000477.6	CCTGCCTGTTGCCAAAGCTCGAT	TGGCTCAGGCGAGCTACTGC
APOA2	NM_001643.1	AGCCTTGAAGGAGCTTTGGTTCGG	ACTGGGTGGCAGGCTGTGTTC
APOB	NM_000384.2	CCTGGGGCAGTGTGATCGCT	TGACAAGGGGCGGGTCATGC
APOC1	NM_001645.4	TCCTGTCGCTCCCGGTCCTG	GAAAACCACTCCCGCATCTTGGC
APOE	NM_001302688.1	CCAGGAGCCGGTGAGAAGCG	TGTGATTGGCCAGTCTGGAGGC
CDX2	NM_001265.4	CGGCAGCCAAGTGAAAACCAGG	TCGGCTTTCCTCCGGATGGTG
CYP3A4	NM_017460.5	CCCAGCAAAGAGCAACACAGAGC	CAGAGGTGTGGGCCCTGGAAT
GATA4	NM_001308093.1	GCAGAGAGTGTGTCAACTGTGGGG	TGGGGACCCCGTGGAGCTT
HHEX	NM_002729.4	ACACGCACGCCCTGCTCCGC	TGGCCAGACGCTTCCTCTCGGGC
HLXB9	NM_005515.3	GCGTCCACCGCGGGCATGATCC	AAGCGCTTGGGCCGCGACAGG
HNF1A	NM_001306179.1	CTTCTGCAGGAGGACCCGTGGCGT	GGCGGCCCGCTTCTGCGTCT
HNF1B	NM_000458.3	GGGGCCCGCGTCCCAGCAAA	GGCCGTGGGCTTTGGAGGGGG
HNF4A	NM_000457.4, NM_175914.4	GGACGACCAGGTGGCCCTGCTCAGA	GCTCCGGGCAGTGCCGAGGGA
HNF4A (P1)	NM_000457.4	GTGTTGACGATGGGCAATGACACG	CATGCCAGCCCGGAAGCATT
HNF4A (P2)	NM_175914.4	CAGTGGAGAGTTCTTACGACACG	CTTCTTCGCCCGAATGTCGC
HOXA10	NM_018951.3	TCCCTGGGCAATTCCAAAGGTGAAA	AGGTGGACGCTGCGGCTAAT
HOXA11	NM_005523.5	TTCCGGCCACACTGAGGACAAG	GTTGAGCATGCGGGACAGTTGC
HOXA13	NM_000522.4	CACTCTGCCCGACGTGGTCTC	ACCTTGGTATAAGGCACGCGCT
HOXC10	NM_017409.3	CCTCGGATAACGAAGCGAAAGAGGA	TCTTGCTAATCTCCAGGCGGCG
HOXC11	NM_014212.3	CGCAGATTTCGGCGAGCGAG	TGGTGCCACTTGCCGGATGG
HOXC12	NM_173860.1	GGGGCCGCTGGTAAACATCCA	GGCGTGGGTAGGACAGCGAA
HOXD11	NM_021192.2	ATGCTCAACCTCACTGACCGGC	GGCGCTTCCTGGAGCTCTCAAA
HOXD12	NM_021193.3	AGCGGAAACCCTACACGAAGCA	TGACTTGCTGGTCGCTGAGGTTC
HOXD13	NM_000523.3	GCTACCACTTCGGCAACGGCTAC	GGCACGTGCTGGTAAGGGCTC
INS	NM_000207.2	CCTGCAGGTGGGGCAGGTGGAGC	CGGGTGTGGGGCTGCCTGCG
KCNJ11	NM_000525.3	AGTGGGACCCAGGTGGAGGT	GTGGCCTAGGGCCTCACTGC
MAFA	NM_201589.3	GCCCGCTGGCCATCGAGTACGTCA	GAGGACAGCGAGCCTGGCGGC
NKX6.1	NM_006168.2	ACGCACGCCTGGCCTGTACCCC	CCCTCTCGGGCCCCGCCAAGTA
PDX1	NM_000209.3	CCTTCCCGGAGGGAGCCGAGCC	GTAGGCCGTGCGCGTCCGCT
RFX6	NM_173560.3	GCGGCTTGGAACAAGAGGCCA	ACGAGTGAAGCCACCCTCATTCTTT
SOX9	NM_000346.3	ACCAGCCGCGGCGGAGGAAGT	GGGATTGCCCCGAGTGCTCGCC

TRANSPARENT METHODS

Generation of hiPSCs

5 x 10^5 human fibroblast cells were seeded on a 6-well plate prior to transduction. After 24 hours, cells were replenished with medium containing non-integrative Sendai reprogramming vectors (polycistronic Klf4–Oct3/4–Sox2, L-Myc, and Klf4) according to the CytoTune-iPS 2.0 Sendai Reprogramming Kit (Thermo Scientific). All experiments with hiPSCs were approved by the Regional Committee of Medical and Health Research Ethics (REK 2010/2295), and all methods were performed in accordance with the Helsinki Declaration.

Human PSC culture and differentiation

HiPSCs generated from human fibroblast cells and H9 cells were at cultured at 37°C with 5% CO_2 in DMEM/F-12 with 15 mM HEPES (STEMCELL Technologies), 20% KnockOut™ serum replacement (KOSR), L-glutamine, NEAA (Life Technologies) and supplemented with 10 ng/ml FGF2 (Miltenyi Biotec). HiPSCs were seeded on irradiated CF-1 mouse embryonic fibroblasts (MEFs) and hiPSC media was replaced every 24 hours.

HiPSCs or H9 cells were differentiated into HPPs as described previously (Teo et al., 2012), with some modifications. Briefly, cells were incubated with Dispase (STEMCELL Technologies) and Collagenase IV (Life Technologies) and collected by mechanical scraping. MEFs were removed by passing the suspension through a 70 µm cell strainer. Plated cells were differentiated 2 days later in RPMI-1640/2% B-27 (no vitamin A; serum-free chemically-defined medium) supplemented with 100 ng/ml Activin A (R&D Systems), 3 µM CHIR99021 (Tocris) and 10 µM LY294002 (LC

Labs). On day 3, differentiation medium containing 50 ng/ml Activin A was added. On day 5, differentiation medium containing 50 ng/ml FGF2 (Miltenyi Biotec), 3 μM all-trans-retinoic acid (RA) (WAKO), and 10 mM nicotinamide (Sigma) was added, followed by subsequent media changes and addition of 20 μM DAPT (Abcam) on days 10 and 12.

HiPSCs and H9 cells were differentiated into hepatocyte-like cells as described previously (Hannan et al., 2013), with some modifications. The basal differentiation media used was the same as that for the HPP differentiation protocol described above during the first 9 days. The same supplements were also used for the first 4 days of differentiation. On day 5, differentiation medium containing 50 ng/ml Activin A was added. From days 6-9, differentiation media supplemented with 20 ng/ml BMP4 (Miltenyi Biotec) and 10 ng/ml FGF10 (Miltenyi Biotec) was added and replaced daily. From days 10-24, the HCM Bulletkit (Lonza) differentiation media supplemented with 30 ng/ml Oncostatin M (Miltenyi Biotec) and 50 ng/ml HGF (Miltenyi Biotec) was added and replaced every other day.

HiPSCs and H9 cells were differentiated into β-like cells as described previously (Pagliuca et al., 2014), with some modifications. Cells were dissociated using Dispase (STEMCELL Technologies Inc) and Collagenase IV (Life Technologies), followed by mechanical scraping. MEFs were removed by passing the suspension through a 40 μm cell strainer. TrypLE Express (Life Technologies) was added for further dissociation into single cells. 1 x 10^6 single cells in mTeSR1 (STEMCELL Technologies Inc) containing 10 μM of Rho-Kinase Inhibitor (Y27632) (STEMCELL Technologies Inc) were seeded into each well of a Corning® CoStar® ultra-Low attachment 6-well plate. After 24 hours, media was replaced with mTeSR1 without

Y27632 and cells were cultured for another 48h before initiation of differentiation (Pagliuca et al., 2014).

In general, 1–3 independent hiPSC lines per subject were used in experiments, with biological triplicates analysed for each line. Experiments were repeated at least thrice.

All hPSC lines used were tested mycoplasma-negative.

FGF2 dose-response treatments

H9 cells were differentiated into day 5 cells following the HPP differentiation protocol as described above. On day 5 onwards, cells were treated with differentiation medium containing increasing doses of FGF2 (Miltenyi Biotec) – 50 ng/ml, 100 ng/ml, 200 ng/ml, 300 ng/ml till day 14 before being harvested for analysis (Ameri et al., 2010).

Clonal cell line culture

HepG2 cells were purchased from ATCC (HB-8065) and cultured in DMEM/Low glucose (Hyclone) with 10% heat-inactivated FBS (Life Technologies) and 1% NEAA (Life Technologies). EndoC-βH1 cells (Ravassard et al., 2011) were purchased from Univercell Biosolutions and cultured in DMEM/Low glucose (Life Technologies) supplemented with BSA (Sigma Aldrich), penicillin/streptomycin, 2 mM L-glutamine, 50 µM 2-mercaptoethanol, 10 mM nicotinamide (Sigma Aldrich), 5.5 µg/ml transferrin (Sigma Aldrich) and 6.7 ng/ml sodium selenite (Sigma Aldrich) on plates coated with 2 µg/ml fibronectin (Sigma Aldrich) and 1% ECM (Sigma Aldrich). Ad293 cells were cultured in DMEM/High glucose (Hyclone) with 10% heat-inactivated FBS (Life Technologies) and 1% NEAA (Life Technologies).

All cell lines used were tested mycoplasma-negative.

Immunofluorescence staining

Cell clumps were collected at the end of the differentiation and cryo-embedded in tissue freezing medium (Leica Biosystems). Cryo-embedded cells were sectioned and mounted onto glass slides. Sectioning was performed by the Advanced Molecular Pathology Laboratory (AMPL), A*STAR and stored at -80 °C. Cell sections or cells in monolayer culture were fixed with 4% paraformaldehyde for 20 minutes, permeabilised with 0.1% Triton X-100 in DPBS, then blocked with 5% donkey serum or 5% bovine serum albumin in DPBS containing 0.1% Triton X-100, before overnight incubation with primary antibodies at 4^{o}C. Primary antibodies used are for the detection of HNF4A (C-terminal epitope, Santa Cruz, sc-6556), HNF4A (N-terminal epitope, Abcam, ab181604), FLAG tag (Sigma Aldrich, F1804), HOXC10 (Abcam, ab153904), HOXC12 (Life Technologies, MA5-19125), SOX17 (R&D, AF1924), CXCR4 (BD Biosciences, 555976), PDX1 (R&D, AF2419), GATA4 (Thermo Fisher Scientific, MA5-15532) and C-peptide (DSHB, GN-ID4). Secondary antibody incubation was carried out followed by staining with DAPI. The secondary antibodies used were Alexa Fluor® 488 (Invitrogen, A11055), Alexa Fluor ® 488 (Invitrogen, 21202), Alexa Fluor® 594 (Invitrogen, A21203) or Alexa Fluor® 488 (Invitrogen, A21270). Brightfield images were acquired with the Axiovert 200M inverted microscope using the Axiovision LE software. Confocal images were acquired with the Olympus FV1000 inverted confocal microscope using the Olympus Fluoview v3.1 software.

Fluorescence-activated cell sorting (FACS)

Cells were harvested by mechanical scraping and dissociated into single cells following incubation with 0.25% Trypsin/EDTA at 37°C and passed through a 40 µm cell strainer. Cell clumps were dissociated into single cells using TrypLE Express (Life Technologies) at 37°C and passed through a 40 µm cell strainer. Single cells were fixed with 4% paraformaldehyde on ice for 1 hour, then blocked in FACS buffer (5% FBS in DPBS) containing 0.1% Triton X-100 on ice for 1 hour, followed by incubation with primary antibodies for 1 hour at 4°C. Primary antibodies used are for the detection of HNF4A (C-terminal epitope, Santa Cruz, sc-6556), HNF4A (N-terminal epitope, Abcam, ab181604), SOX17-PE (R&D, IC19241P), CXCR4-APC (BD Biosciences, 555976), PDX1 (Abcam, ab47308) and INS (Abcam, ab7842). Cells were washed with FACS buffer containing 0.1% Triton X-100 cells and incubated with secondary antibodies in the dark for 1 hour at 4°C. The secondary antibodies used were Alexa Fluor® 488 (Invitrogen, A11055), Alexa Fluor ® 488 (Invitrogen, 21202) or Alexa Fluor® 594 (Invitrogen, A11076). Finally, cells were washed in FACS buffer, resuspended in DPBS and analysed with the BD™ LSR II Flow Cytometer. Data analysis was performed using the FlowJo 7.0 software.

RNA extraction, reverse transcription and quantitative PCR

PrepEase RNA Spin Kit (Affymetrix) was used to extract total RNA from differentiated hiPSCs according to the manufacturer's instructions. To remove genomic DNA from the preparation, DNase treatment was carried out for 15 minutes at room temperature. Purified RNA was reverse transcribed using the High-Capacity cDNA Reverse Transcription Kit (Applied Biosystems). QPCR was performed on the CFX384 Touch™ Real-Time PCR Detection System with iTaq™ Universal

SYBR® Green Supermix (Bio-Rad). Reported fold changes are based on relative expression values calculated using the $2^{-\Delta\Delta C(T)}$ method with normalization to actin expression for each sample. QPCR primers were custom-designed to span exon-exon junctions, wherever possible, using Primer-BLAST (NCBI). Sequences of primers used are listed in Table S2.

Immunoblotting

Cells were harvested by mechanical scraping on ice and lysed in M-PER (Thermo Scientific) in the presence of protease and phosphatase inhibitors (Sigma Aldrich). Protein lysates were quantified using the BCA Assay (Thermo Scientific), separated with sodium dodecyl sulphate polyacrylamide gel electrophoresis (SDS-PAGE) using the Mini-PROTEAN Tetra Cell system (Bio-Rad) and transferred to PVDF membranes (Bio-Rad). Primary antibodies against endogenous HNF4A protein (Cell Signaling, 3113), FLAG tag (Sigma Aldrich) or actin (Sigma Aldrich) were used, followed by HRP-conjugated secondary antibodies (Santa Cruz). Chemiluminescent signals were detected using Super Signal West Dura Extended Duration substrate (Thermo Scientific).

Generation of expression constructs

The pCDH plasmid (System Biosciences) containing the CMV promoter, N-terminal FLAG tag coding sequence and ampicillin resistance gene was used as the expression vector for HNF4A2 and HNF4A8. HNF4A2 coding sequence was amplified from cDNA obtained from control D14 HPPs using the following primers: Forward primer 5’ ATGCGACTCTCCAAAACCCTC 3’; Reverse primer: 5’ CTAGATAACTTCCTGCTTGGTGA 3’. HNF4A8 coding sequence was amplified

from cDNA obtained from human islets (University of Alberta) using Phusion polymerase (Thermo Scientific) and the following primers: Forward primer 5' ATGGTCAGCGTGAACGCG 3'; Reverse primer: 5' CTAGATAACTTCCTGCTTGGTGA 3'. PCR products were inserted into the pCDH vector using the Quick Ligation Kit (NEB). The ligated plasmid was used to transform STBL3 competent cells (Thermo Fisher Scientific). Inserted sequences were verified by DNA sequencing. For site-directed mutagenesis, the following primers were used to generate the p.Ile271fs mutation by introducing an additional adenine base into the HNF4A coding sequence through a PCR using the Phusion polymerase (Thermo Scientific): Forward primer 5' CTCAAAGCCATCAATCTTCTTTGACC 3'; Reverse primer: 5' GTAGGCATACTCATTGTCATCGATC 3'. The parental strand was digested following incubation with *Dpn1* (NEB). Introduced mutations were verified by DNA sequencing.

Luciferase reporter assays

The h*HNF1A* promoter (-605 to +18) and h*APOB* promoter (-664 to +7) were cloned into the pGL4.10 vector. The h*AFP* enhancer region (-4730 to -3666) containing the HNF4A binding site was cloned into pGL4.23-Promoter vector. The h*HNF4A* P1 and P2 promoter constructs in the pGL4.10 vector were described previously (Teo et al., 2016). Cell lines or differentiated hiPSCs were co-transfected with the respective promoter construct, pRL-TK renilla vector, and an overexpression vector (Empty pCDH or pCDH-HNF4A WT or mutant) using Fugene 6 transfection reagent (Promega) or Lipofectamine 2000 (Life Technologies). Cells were transfected in triplicate wells and each experiment was independently performed at least twice. For *HNF4A* knockdown in EndoC-βH1 cells, siRNA-mediated RNA interference was

carried out using 25 nM non-targeting (D-001810-10) or *HNF4A*-targeting (J-003406-09) ON-TARGETplus human siRNA (Dharmacon, GE Healthcare) with Lipofectamine RNAiMAX (Life Technologies) for 48 hours before transfection for luciferase experiments. Cells were harvested 24-48h after transfection, and luciferase activity was measured using the Dual Luciferase Assay System (Promega). Firefly luciferase activity was normalized to Renilla luciferase activity for each well.

Chromatin immunoprecipitation (ChIP)

EndoC-βH1 cells from 2 confluent 10 cm plates were cross-linked with 3.3 mg/ml of dimethyl 3,3'-dithiobispropionimidate and 1 mg/ml of 3,3’-dithiodipropionic acid di(N-hydroxysuccinimide ester) (both Sigma Aldrich) for 30 minutes at room temperature and with 1% formaldehyde (Amresco) for 15 minutes. The cross-linking reaction was quenched with 0.125 M glycine and cells were first lysed in cell lysis buffer (10 mM Tris-HCl pH 8, 10 mM NaCl and 0.2% NP-40) and then in nuclear lysis buffer (50 mM Tris-HCl pH 8, 10 mM EDTA and 1% SDS) on ice in the presence of protease inhibitors on ice. Nuclear lysates were diluted in IP dilution buffer (20 mM Tris-HCl pH 8, 2 mM EDTA, 150 mM NaCl, 0.01% SDS and 1% Triton X-100) and sonicated for 30s on/45s off for 10 cycles using a Q500 sonicator (QSonica) with microtip probes at 30% power. Sonicated samples were pre-cleared using 10 µg rabbit IgG (Santa Cruz) and Protein A/G agarose beads. Agarose beads were removed by centrifugation and a portion of the supernatant was collected as the input control. Samples were divided equally and incubated with 10 µg of HNF4A antibody (Santa Cruz, sc-8987) or rabbit IgG overnight at 4°C. The following day, samples were incubated with Protein A/G agarose beads and the beads were recovered and

washed with IP wash buffer and Tris-EDTA buffer. The immunoprecipitated DNA was eluted from the beads using IP elution buffer (100 mM NaHCO3, 1% SDS, 100 mM DTT). Samples were successively treated with RNaseA, NaCl and Proteinase K. DNA was extracted by phenol/chloroform extraction. Finally, qPCR was carried out on the input, HNF4A pulldown and IgG samples using SYBR green (Bio-Rad), targeting the *HNF1A* promoter or a control region in *GAPDH*. QPCR data were quantitated using a standard curve based on the input DNA, and normalized against *GAPDH*. Results are expressed as fold change for *HNF4A* pulldown relative to IgG control.

RNA sequencing and differential expression analysis

Poly-A mRNA was enriched from 1 µg of total RNA with oligo-dT beads (Invitrogen). Up to 100 ng of poly-A mRNA recovered was used to construct multiplexed strand-specific RNA-seq libraries as per manufacturer's instruction (NEXTflex^{TM} Rapid Directional RNA-SEQ Kit, dUTP-Based, v2). Individual library quality was assessed with an Agilent 2100 Bioanalyzer and quantified with a QuBit 2.0 fluorometer before pooling for sequencing on a HiSeq 2000 (1 x 101 bp read). The pooled libraries were quantified using the KAPA quantification kit (KAPA Biosystems) prior to cluster formation. Adapter sequences and low quality bases in Fastq read sequences were trimmed using Trimmomatic (v.0.33) (parameters: LEADING:3 TRAILING:3 SLIDINGWINDOW:4:15 MINLEN:36). The quality filtered Fastq sequence reads were then aligned to the human genome (hg19) using Tophat (v.2.0.14) (parameters: --no-coverage-search --library-type=fr-firststrand) and annotated with Ensembl gene IDs. The resulting bam files were used to generate feature read counts using the Python package-based htseq-count of HTSeq (v.0.6.1p1) (parameters: default union-

counting mode, --stranded=reverse). The read count matrix output from HTSeq was used to perform differential expression analysis using the edgeR package (available in R (v.3.1.3)) in both 'classic' and generalized linear model (glm) modes to contrast patient versus control. Procedures described in edgeR documentation were followed to calculate P-values, FDR adjusted p-values (q-values) and fold-changes. A false discovery rate (FDR) cutoff of 0.05 was used to filter significantly differentially expressed genes. These genes with Ensembl IDs were mapped to gene symbols.

Allele-specific qPCR

A custom TaqMan® assay (Applied Biosystems) was designed to target the human *HNF4A* mRNA sequence surrounding the p.Ile271fs mutation (Assay ID: ANRWJVF). QPCR was performed on the CFX384 Touch™ Real-Time PCR Detection System (Bio-Rad) using the TaqMan® SNP Genotyping MasterMix (Applied Biosystems), according to the manufacturer's protocol. An allelic discrimination plot was generated on R using relative luciferase units (RFU) from the HEX (WT allele) and FAM (Mutant allele) probes.

Statistical analysis

Statistical parameters, number of replicates (n) and independent experiments conducted are indicated in the figure legends. Data represent mean ± SD. Gene expression and ChIP qPCR data were analyzed using two-tailed unpaired Student's *t*-test. Luciferase data were expressed as normalized relative Firefly/Renilla luciferase activity. Mean differences in relative activity were analyzed using two-tailed paired Student's *t*-test for clonal cell line studies, while two-way ANOVA with Bonferroni post tests (GraphPad Prism) was used for hiPSC-based studies to

analyze differences in relative activity segregated by MODY1 status and overexpression condition. Immunofluorescence data was quantified by cell counting using ImageJ across at least three representative images per condition. Results were considered to be significant at $P<0.05$.

Data and software availability

The accession number for the RNA-Seq data reported in this paper is GEO: GSE106335.

SUPPLEMENTAL REFERENCES

Ameri, J., Stahlberg, A., Pedersen, J., Johansson, J.K., Johannesson, M.M., Artner, I., and Semb, H. (2010). FGF2 specifies hESC-derived definitive endoderm into foregut/midgut cell lineages in a concentration-dependent manner. Stem Cells *28*, 45-56.

Hannan, N.R., Segeritz, C.P., Touboul, T., and Vallier, L. (2013). Production of hepatocyte-like cells from human pluripotent stem cells. Nature protocols *8*, 430-437.

Pagliuca, F.W., Millman, J.R., Gurtler, M., Segel, M., Van Dervort, A., Ryu, J.H., Peterson, Q.P., Greiner, D., and Melton, D.A. (2014). Generation of Functional Human Pancreatic beta Cells In Vitro. Cell *159*, 428-439.

Ravassard, P., Hazhouz, Y., Pechberty, S., Bricout-Neveu, E., Armanet, M., Czernichow, P., and Scharfmann, R. (2011). A genetically engineered human pancreatic beta cell line exhibiting glucose-inducible insulin secretion. J Clin Invest *121*, 3589-3597.

Teo, A.K., Lau, H.H., Valdez, I.A., Dirice, E., Tjora, E., Raeder, H., and Kulkarni, R.N. (2016). Early Developmental Perturbations in a Human Stem Cell Model of MODY5/HNF1B Pancreatic Hypoplasia. Stem Cell Reports *6*, 357-367.

Teo, A.K.K., Ali, Y., Wong, K.Y., Chipperfield, H., Sadasivam, A., Poobalan, Y., Tan, E.K., Wang, S.T., Abraham, S., Tsuneyoshi, N*., et al.* (2012). Activin and BMP4 Synergistically Promote Formation of Definitive Endoderm in Human Embryonic Stem Cells. STEM CELLS *30*, 631-642.